

Article

# Canopy Urban Heat Island and Its Association with Climate Conditions in Dubai, UAE

Afifa Mohammed <sup>1,\*</sup>, Gloria Pignatta <sup>1</sup> , Evangelia Topriska <sup>2</sup>  and Mattheos Santamouris <sup>1</sup>

<sup>1</sup> Faculty of Built Environment, University of New South Wales (UNSW), Sydney, NSW 2052, Australia; g.pignatta@unsw.edu.au (G.P.); m.santamouris@unsw.edu.au (M.S.)

<sup>2</sup> Department of Architectural Engineering, Faculty of Energy, Geoscience, Infrastructure and Society, Heriot-Watt University, Dubai International Academic City, Dubai 294345, UAE; e.topriska@hw.ac.uk

\* Correspondence: a.mohammed@student.unsw.edu.au

Received: 25 May 2020; Accepted: 24 June 2020; Published: 26 June 2020



**Abstract:** The impact that climate change and urbanization are having on the thermal-energy balance of the built environment is a major environmental concern today. Urban heat island (UHI) is another phenomenon that can raise the temperature in cities. This study aims to examine the UHI magnitude and its association with the main meteorological parameters (i.e., temperature, wind speed, and wind direction) in Dubai, United Arab Emirates. Five years of hourly weather data (2014–2018) obtained from weather stations located in an urban, suburban, and rural area, were post-processed by means of a clustering technique. Six clusters characterized by different ranges of wind directions were analyzed. The analysis reveals that UHI is affected by the synoptic weather conditions (i.e., sea breeze and hot air coming from the desert) and is larger at night. In the urban area, air temperature and night-time UHI intensity, averaged on the five year period, are 1.3 °C and 3.3 °C higher with respect to the rural area, respectively, and the UHI and air temperature are independent of each other only when the wind comes from the desert. A negative and inverse correlation was found between the UHI and wind speed for all the wind directions, except for the northern wind where no correlation was observed. In the suburban area, the UHI and both temperatures and wind speed ranged between the strong and a weak negative correlation considering all the wind directions, while a strong negative correlation was observed in the rural area. This paper concludes that UHI intensity is strongly associated with local climatic parameters and to the changes in wind direction.

**Keywords:** subtropical desert climate; urban overheating; cluster analysis; air temperature; wind speed and wind directions; synoptic conditions

## 1. Introduction

As observed in many cities globally, rapid urbanization has produced negative effects on the climate and the local microclimate. Currently, the urban population exceeds 50% of the total of the world's population and by 2050 it is expected to rise above 60%. This means that with urban development worldwide and at the current rate of population growth, another 2.5 billion people will be living in urban areas by 2050 [1]. Consequently, this urban expansion will exacerbate the hostile impact that human activities are already having on environmental systems.

Rapid urbanization has boosted regional climate change. In particular, the increase in urban heat island (UHI) intensity is strictly connected with the urbanization growth given the derived increase in anthropogenic heat emissions, land-use change (with the associated decrease in the vegetation and the albedo of the built area), and changes in the advection.

The UHI phenomenon has been documented in more than 400 cities around the world [2]. Its impact is closely related to land cover which controls the energy budget on the earth's surface. The surface

energy budget difference between the urban and rural zone, caused by various thermal-optical surface characteristics, leads to the occurrence of the UHI phenomenon [3]. Thus, urban areas are hotter than their undeveloped surroundings. This phenomenon has a significant impact not only on the environmental quality of cities, but also on energy, thermal comfort, and health [4–7]. In particular, the UHI increases the demand for peak-time electricity and the consumption of cooling energy in buildings, intensifies the concentration of various harmful pollutants, increases the ecologically harmful footprint of cities, and has a significant impact on health [8]. Most cities are sources of pollution and heat, released from buildings and roads. The manifestation of the UHI phenomenon is influenced by several factors including climate variables (i.e., air temperature, air relative humidity, wind speed) and the related local synoptic weather conditions [9,10], thermal-optical characteristics of the materials, the magnitude of the anthropogenic heat released, and the existing heat sources in the areas [2].

On the other hand, the construction and building industries are indispensable to everyday life and are essential to future social and technological developments. However, they are responsible for a great deal of pollution, generation of waste, and the consumption of energy and natural resources accounting for 30%–40% of the overall consumption on the planet [11,12]. Moreover, these industries have negative effects on the local and global climate [12]. The International Energy Agency estimates that the growth in energy consumption will be around 38.4 PWh in urbanized countries by 2040, while energy consumption globally was about 23.7 PWh in 2010 [13]. These industries account for 38% of all greenhouse gas emissions. They also contribute significantly to increase the temperature of cities by producing the urban heat island (UHI) phenomenon [8].

Population growth and rural depopulation will lead to greater energy consumption, particularly in hot and dry cities which require more cooling loads; in addition, this increases the number of gas emissions and pollution that negatively interact with the phenomenon of the UHI [14]. Furthermore, the expansion of urban areas will require a more complex energy infrastructure to meet demand [12,15].

Recently, many studies have demonstrated that per degree of temperature increase, the peak electricity demand increases by between 0.45% and 4.6% due to the UHI [16]. Moreover, it is expected that by 2050, there will be a massive increase of about 750% and 275% globally in the cooling requirements of the residential and commercial sectors, respectively [17]. Furthermore, the UHI has a significant impact on human health, as several studies have shown that high temperatures lead to a great increase in the number of people suffering from heat exhaustion and heatstroke in urban areas [18]. Moreover, it has been pointed out that there is a strong correlation between the increase in human mortality and the rise in urban temperatures [19]. Several studies in various Asian cities have shown that temperatures above 29 °C can increase the mortality rate between 4.1% and 7.5% per 1 °C increase in temperature [20]. Hence, from the aforementioned discussion, it is clear that cities need specific controls and strategies to mitigate the negative impacts of the UHI phenomenon [12].

Among the performed studies on UHI, three different definitions of UHI are usually considered, such as the boundary UHI for mesoscale analysis [21], the canopy UHI for microscale analysis [22], and the surface UHI [23]. Different methods have been reported [24] to identify the different UHI types, including direct and indirect methods, numerical modeling, and estimates based on empirical models.

In contrast with the numerous studies on UHI performed in temperate regions, only a few studies have been concentrated in the observation of the UHI intensity in desert regions [25,26]. Some of those studies state that the UHI presents a diurnal and seasonal cycle in the Gulf area. The canopy level of the UHI of Muscat, Oman, reaches the peak approximately 7 h after sunset based on summer meteorological observations. Muscat city is characterized by low ventilation, many business activities, multi-storied buildings, heavy traffic, and topography factors [27]. In another study in Bahrain, numerical modeling was performed and the results show an increase in the simulated average air temperature of about 2 °C–5 °C when assessing the impact of the urbanization and that the canopy UHI magnitude is enhanced by various urban activities such as construction processes, vegetation shrinkage, and sea reclamation [28].

Given the lack of information about UHI intensity concepts in the Middle East in general [28] and specifically in Dubai, United Arab Emirates (UAE), this paper aims to quantify and analyze the intensity of the canopy UHI in Dubai, highly influenced by the urban geometry and physical properties of the built environment, and its relation with the main climatic parameters continuously monitored for a period of five years.

## 2. Materials and Methods

### 2.1. Geographical Location, Population, and Climate of Dubai

Dubai, one of the seven emirates and the second largest city of the United Arab Emirates (UAE), has an area of 4114 km<sup>2</sup>, accounting for 5% of the overall area of the country. Dubai city is recognized as the economic capital of the UAE. Situated on the Tropic of Cancer, between 25°16' N and 55°18' E, it has a coastal length of 72 km on the eastern coast of the Arabian Peninsula and faces the South-West of the Arabian Gulf [29,30].

According to the census conducted by the Statistics Centre of Dubai, Dubai is the city with the highest population density in the UAE. The population of Dubai increased by 27% from 2,327,350 to 3,192,275 between 2014 and 2018 inclusively [31].

The Dubai region has a subtropical desert climate, with hot and humid summers and warm winters [30]. The air temperature ranges between 10 °C to 30 °C in the winter season and increases up to 48 °C in the summer season [29]. The hot period starts with average daily temperatures over 37 °C from 18 May to 23 September, lasting for 4.1 months; the cool season starts with average temperatures of less than 27 °C from December 4th to March 8th and lasts for 3.1 months [32]. Winter is characterized by rainfall and fog, while in summer, the relative humidity reaches 80%–90% [29]. The average rainfall ranges between 13 and 17 mm [32].

### 2.2. Meteorological Stations and Data Analysis

In this study, climate data (i.e., air temperature, relative humidity, wind speed, and wind direction) were collected by three meteorological stations in Dubai (i.e., Dubai International Airport station, Al-Maktoum International Airport station, and Saih Al-Salem Station) belonging to the UAE National Center of Meteorology (NCM). Hourly data of each microclimate parameter were collected from each meteorological station and analyzed in the MS Excel tool for a period of five years from 2014 to 2018 (i.e., 43,824 values recorded in total for each climate variable). Data of cloud coverage were also collected by the two stations of Dubai Airport and Al-Maktoum Airport, while the solar radiation that equally affects the three areas of Dubai was not measured by any meteorological station. In this study, no further tools were used for the data analysis except for MS Excel.

Table 1 summarizes the geographical information of the three meteorological stations [33], while Figure 1 shows their locations in Dubai. All three stations are installed at a height of about 10 m from the ground, allowing to perform the microscale analysis of the UHI phenomenon, investigating the canopy UHI and its association with the climate parameters measured at the same height.

Station 1 (Table 1) is located within Dubai International Airport, one of the largest and most modern airports in the world, located in Al Garhoud City, which is a commercial and residential region of Dubai, approximately 5 km (2.9 miles) East of the Dubai's CBD (central business district), and around 19 m above sea level [34]. A total of 15,000 solar panels were installed on the roof of the airport building 2 km away from the meteorological station [35].

Station 2 (Table 1) is located within the Al Maktoum International Airport, 37 km (23 miles) South-West of Dubai. The airport is surrounded by a mixed-use area, made of residential and commercial buildings; it is the major part of the Dubai World Central in the Jebel Ali zone with a total area of around 14,000 hectares (35,000 acres). This area could be described as an open area. It is almost at a 16 km (10 miles) distance from the sea and has no surrounding buildings or major obstacles that could interfere with the wind flowing from different directions [36].

Station 3 (Table 1) is located within Saih Al Salem, a village in Dubai with a population of 589 residents, accounting for 0.02% of the total population of Dubai, as reported by the Dubai Statistic Centre in 2018 [37]. The meteorological station is surrounded by the Marmoom Desert Conservation Reserve, which constitutes 10% of the total area of Dubai. It is the first unfenced desert reserve in the UAE. The total area exceeds 40 hectares of shrubland and contains many lakes with a total area of around 10 km<sup>2</sup> [38]. The amount of vegetation in the areas surrounding the three stations is negligible.

In Table 1, the population density of the three locations is calculated as the ratio between the population and the land area of the sectors of Dubai to which the weather stations belong. Considering as references the population densities of Sector 1 (i.e., 10,561/km<sup>2</sup>) classified as “High” and of the Sector 9 (i.e., 5/km<sup>2</sup>) classified as “Low”, then Sector 2, the sector where the weather station of Dubai International Airport is located, is classified as an urban area with a “Medium” population density (3611/km<sup>2</sup>). Al Maktoum International Airport is instead located within Sector 5, presenting a population density of 825/km<sup>2</sup> and therefore classified as a suburban area with a “Medium/Low” population density. The area of Saih Al-Salem presents a low population density of 7/km<sup>2</sup> and being located within Sector 9, was defined as a rural area for this study [39].

**Table 1.** Geographical information and description of the urban, suburban, and rural meteorological stations.

Weather Station No.	Weather Station Name	Latitude (°N)	Longitude (°E)	Station Elevation (m)	Surrounding Area	Population Density (pop./km <sup>2</sup> )
1	Dubai International Airport	25°15'10"	55°21'52"	19	Urban	Medium (3611)
2	Al Maktoum International Airport	24°55'06"	55°10'32"	52	Suburban	Medium/Low (825)
3	Saih Al Salem	24°49'39"	55°18'43"	80	Rural	Low (7)

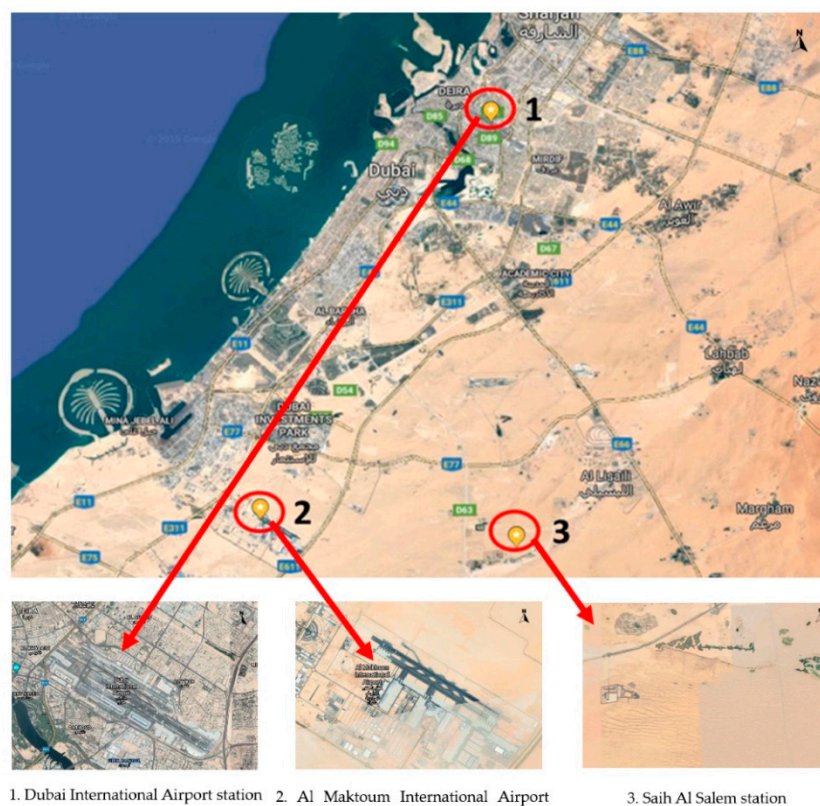


**Figure 1.** Location of the weather stations in Dubai as shown in Google Maps (1. Dubai International Airport station, 2. Al Maktoum International Airport station, 3. Saih Al Salem station).

### 2.2.1. Cluster Analysis of Climate Data

Clustering techniques were used to investigate the level of correlation between the microclimate parameters, i.e., air temperature and wind speed, monitored in the urban and suburban locations, and the canopy UHI intensity under the different ranges of wind directions. The cluster analysis was performed in the MS Excel tool only for the urban and suburban locations because those are the areas where the urbanization may produce an impact on the UHI intensity, while the rural area was considered as the reference location for the calculation of the UHI intensity. The data collected by each meteorological station for the entire period of interest (i.e., 5 years) were divided into six clusters based on the directions of the wind (i.e., either from the seaside or from the desert side, or from the coastal side which is in between, and divided according to four wind direction ranges). The characteristics of the six clusters are summarized in Table 2 and Figure 2.

Table 2. Clusters of wind direction.

Cluster No.	Wind Direction (°)	Directions Specification	No. of Measurements Dubai Airport	No. of Measurements Al Maktoum Airport
1	260–330	The sea	13,689	13,305
2	70–140	The desert	7873	7805
3	200–260	Coastal area	4407	4067
4	140–200	The desert	8848	9320
5	330–20	The sea	4298	4862
6	20–70	Coastal area	4709	4465

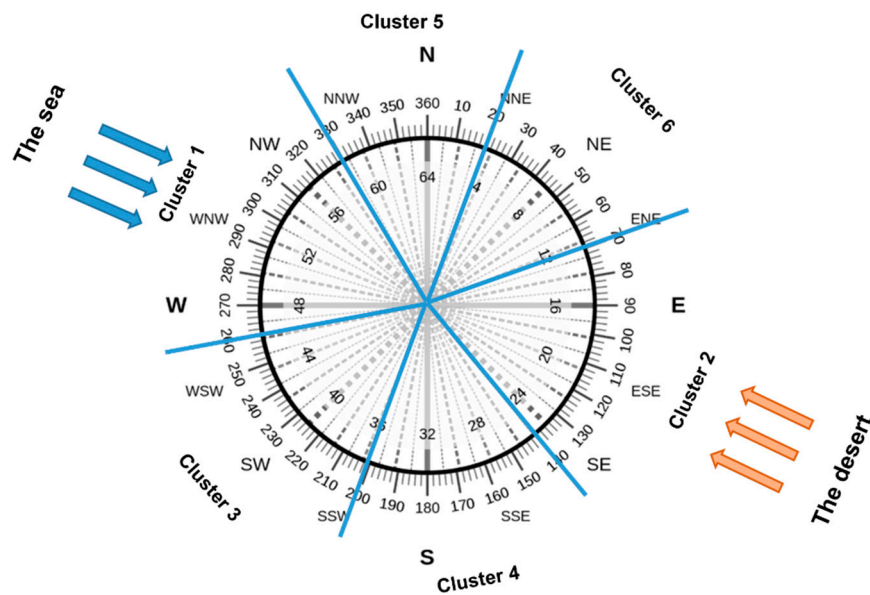


Figure 2. Representation of the six clusters of wind direction.

In Table 2, it can be observed that the dimensions of the six clusters (i.e., number of measurements included in each cluster) are consistent between the urban (i.e., station 1) and the suburban (i.e., station 2) area due to their close proximity. From the cluster analysis, the resulting predominant wind is the one coming from the sea, mainly seen in cluster 1 (i.e., 13,689 and 13,305 for station 1 and station 2, respectively) and cluster 5 (i.e., 4298 and 4862 for station 1 and station 2, respectively). The second predominant wind is the one coming from the desert, mainly seen in cluster 2, but also in cluster 4.

### 2.2.2. Canopy UHI Magnitudes

The hourly canopy UHI magnitude was calculated at 10 m above the ground for the urban and suburban locations for a period of five years (i.e., 2014–2018). Saih Al Salem (i.e., station 3) was chosen

as a reference station, because it is located in a rural area not too far from the downtown city and close to the desert. Of the three stations, this was the least affected by the UHI due to its low level of urbanization. Since this reference station is located outside of the built-up area, it has natural desert coverage and negligible anthropogenic heat.

The canopy UHI magnitude (UHI intensity  $T_{1-T3}$ ) was determined as the air temperature difference between Dubai International Airport (T1 Urban Average) which is station 1 and Saih Al Salem (T3 Rural Average) which is station 3, according to the following equation [40], Equation (1):

$$\text{UHI intensity } T_{1-T3} [^{\circ}\text{C}] = T1 \text{ Urban Average } [^{\circ}\text{C}] - T3 \text{ Rural Average } [^{\circ}\text{C}] \quad (1)$$

While the canopy UHI magnitude (UHI intensity  $T_{2-T3}$ ) was determined by calculating the air temperature difference between Al Maktoum International Airport (T2 Suburban Average) which is station 2 and Saih Al Salem (T3 Rural Average) which is station 3, according to the following equation, [40] Equation (2):

$$\text{UHI intensity } T_{2-T3} [^{\circ}\text{C}] = T2 \text{ Suburban Average } [^{\circ}\text{C}] - T3 \text{ Rural Average } [^{\circ}\text{C}] \quad (2)$$

The canopy UHI calculations, performed according to the above equations, and the data post-processing presented in the result section, were based on the climate data analyzed in MS Excel.

### 3. Results

#### 3.1. Microclimate Analysis

This section presents the microclimate analysis for the three investigated locations in Dubai.

Table 3 summarizes the results of the statistical analysis performed on the main weather parameters (i.e., air temperature, relative humidity, and wind speed) recorded by the three urban, suburban, and rural meteorological stations for the entire period of investigation (i.e., 2014–2018).

**Table 3.** Statistical data of the weather parameters for the three meteorological stations for 5 years (i.e., 2014–2018).

Weather Station No.	Weather Station Name	Weather Parameters	Max Value	Min Value	Average Value	Standard Deviation
1	Dubai International Airport	Temperature dry ( $^{\circ}\text{C}$ )	48.6	12.3	29.6	6.6
		Relative humidity (%)	100	4	50	18.0
		Wind speed (km/h)	63	0	13	6.5
2	Al Maktoum International Airport	Temperature dry ( $^{\circ}\text{C}$ )	48.5	7.1	28.0	7.8
		Relative humidity (%)	100	2	53	22.7
		Wind speed (km/h)	67	0	14	7.9
3	Saih Al Salem	Temperature dry ( $^{\circ}\text{C}$ )	50.8	4.7	28.3	8.9
		Relative humidity (%)	100	1	48	26.0
		Wind speed (km/h)	67	0	10	7.0

Considering the entire 5 year period from 2014 to 2018, the average, maximum, and minimum air temperatures (measured at 10 m above the ground) were 29.6  $^{\circ}\text{C}$ , 48.6  $^{\circ}\text{C}$ , and 12.3  $^{\circ}\text{C}$  for Dubai International Airport station 1, 28.0  $^{\circ}\text{C}$ , 48.5  $^{\circ}\text{C}$ , and 7.1  $^{\circ}\text{C}$  for Al Maktoum International Airport station 2, and 28.3  $^{\circ}\text{C}$ , 50.8  $^{\circ}\text{C}$ , and 4.7  $^{\circ}\text{C}$  for Saih Al Salem station 3, respectively. Station 3 (i.e., Saih Al Salem station), located nearest to the desert, showed the lowest minimum and the highest maximum temperatures (i.e., highest thermal excursion) compared to the other two stations which, being located near the sea, present a local microclimate that is influenced by the Arabic Gulf. The minimum temperatures were recorded by station 3 in February 2014 and 2018 and were lower by about 7.6  $^{\circ}\text{C}$  and 2.4  $^{\circ}\text{C}$  than those recorded by Dubai Airport station and Al Maktoum Airport station, respectively.

In July 2014 and 2017, the maximum temperatures recorded by station 3 were higher by about 2.2 °C and 2.3 °C than those recorded by the stations at Dubai Airport and Al Maktoum Airport, respectively.

Figure 3 summarizes, with the box plot representation, the air temperature measured by the three weather stations for the entire period of investigation (i.e., 2014–2018) and for each year separately.

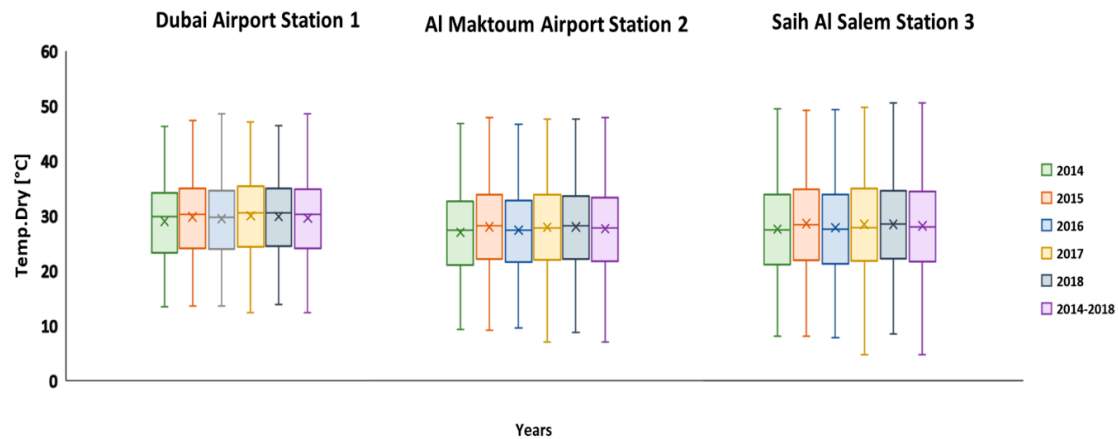


**Figure 3.** Box plot of the air temperature for the urban, suburban, and rural areas in Dubai for 5 years (i.e., 2014–2018).

As expected, each station has an air temperature profile slightly different from the other two, despite their proximity to each other. The different locations of the stations with respect to the desert, the built area, and the coast, produced significant differences in terms of air temperature. The synoptic conditions (i.e., the hot air coming from the desert, the cool air coming from the sea or sea breeze) that characterize the entire area interact in a different way in the proximity of each meteorological station.

According to the collected relative humidity data, which affects the local microclimate, the Summer season is characterized by around 90% humidity. The maximum value recorded in all three stations is 100%, while the minimum and average values range from 1% to 4% and from 48% to 53%, respectively, where as expected, the highest values are experienced in the urban and suburban areas that are located closer to the sea, with a negative impact on human activities and outdoor thermal comfort.

A limited presence of clouds was observed in the urban and suburban areas of Dubai during the monitored period, with a clear annual and seasonal variability of the cloud coverage. In the 5 years of monitoring, the cloud cover rarely reached the maximum value of 9 octas (i.e., sky obstructed from view). Only for 14% and 12% of the time, the sky was between 4 octas (i.e., sky half cloudy) and 9 octas during the monitoring period in the urban and suburban areas, respectively.

In contrast, the total absence of cloud cover (i.e., 0 octas) was recorded very frequently along the monitored period (i.e., 67% and 69% of the time in the urban and suburban areas, respectively) leading to high values of the incident solar radiation, and as a result, to a large amount of the heat absorbed by the built environment during the daytime. This absorbed heat is then released into the atmosphere during the night time. Under these conditions, the nocturnal radiative cooling will be less effective in the built areas with respect to the desert rural area that easily cools down. This contributes to the night-time UHI phenomenon, where the temperature difference between the urban and rural areas is positive at night.

When the sky is completely obstructed from view (i.e., 9 octas), the night-time UHI intensity  $T_{1-T3}$  and  $T_{2-T3}$  reach the maximum (minimum) value of 7.1 °C (0.3 °C) and 3.4 °C (−0.9 °C), respectively, when measured in correspondence to station 1, and of 9.4 °C (0.3 °C) and 7.8 °C (−3.0 °C), respectively, when measured in correspondence to station 2. When the sky is completely clear (i.e., 0 octas), the night-time UHI intensity  $T_{1-T3}$  and  $T_{2-T3}$  reach the maximum (minimum) value of 11.5 °C (−3.3 °C) and 13.0 °C (−7.7 °C), respectively, when measured in correspondence to station 1, and of 11.5 °C (−3.3 °C) and 13.0 °C (−8.9 °C), respectively, when measured in correspondence to station 2. Thus,

the night time UHI variability range is higher under clear sky conditions (i.e., 0 octas) than under cloud-covered sky conditions (i.e., 9 octas). The same result is obtained for the UHI intensity value, as can be observed in Figure 4, which shows the existing relation between the UHI intensity  $T_{1-T3}$  and  $T_{2-T3}$  and the cloud cover for the entire monitored period of 5 years and for the urban and suburban areas.

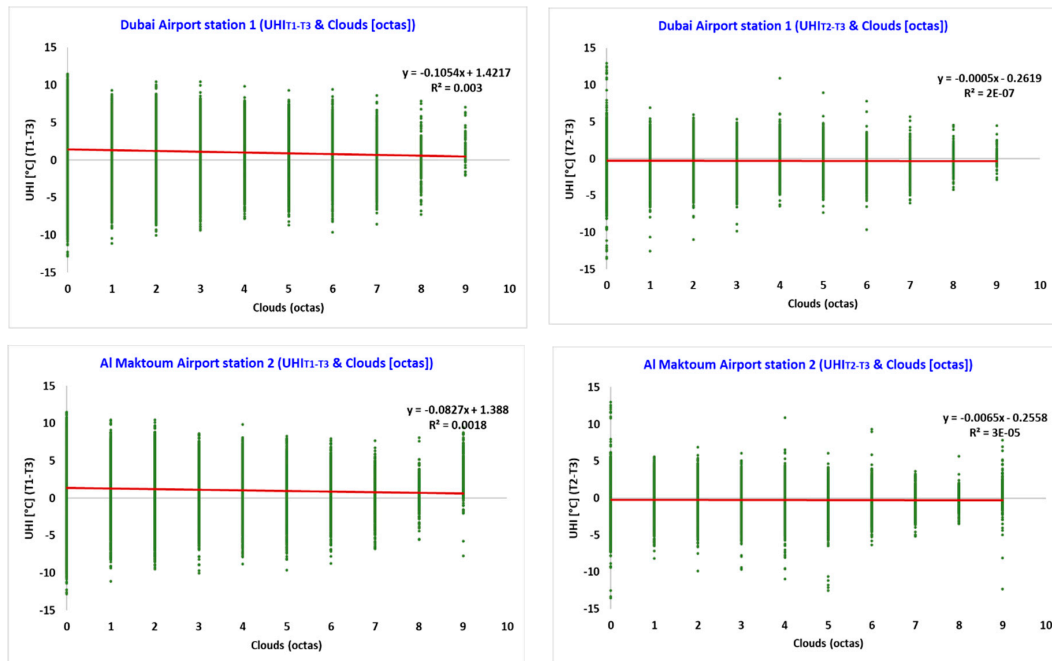


**Figure 4.** Comparison between the urban heat island (UHI) and the cloud cover relation: UHI intensity  $T_{1-T3}$  and cloud cover from station 1 (top left), UHI intensity  $T_{2-T3}$  and cloud cover from station 1 (top right), UHI intensity  $T_{1-T3}$  and cloud cover from station 2 (bottom left), UHI intensity  $T_{2-T3}$  and cloud cover from station 2 (bottom right).

### 3.2. Daytime and Night-Time UHI Intensity and Frequency Distribution

Figure 5 shows the daytime (i.e., 6 a.m.–9 p.m.) and night-time (i.e., 9 p.m.–6 a.m.) boxplot of the canopy UHI intensity  $T_{1-T3}$  and  $T_{2-T3}$  for the entire period of five years considered in this study.

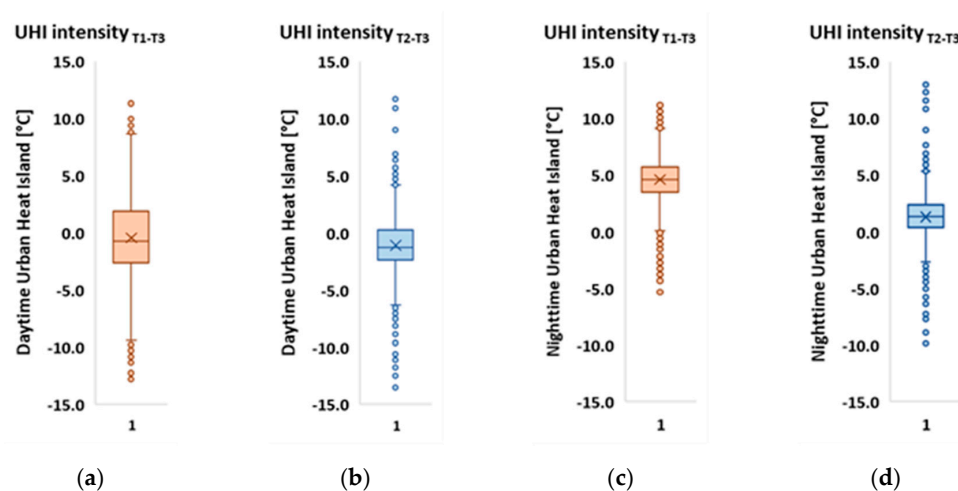


**Figure 5.** Box plot of the daytime and night-time UHI intensity for 5 years (i.e., 2014–2018): (a) daytime UHI intensity  $T_{1-T3}$ , (b) daytime UHI intensity  $T_{2-T3}$ , (c) night-time UHI intensity  $T_{1-T3}$ , (d) night-time UHI intensity  $T_{2-T3}$ .

The daytime and night-time UHI  $T_{2-T3}$  show higher maximum values of 11.7 °C and 13 °C compared to the daytime and night-time UHI  $T_{1-T3}$  values which are 11.3 °C and 11.5 °C, respectively (Figure 5 and Table 4). The average and median values recorded for the daytime and night-time UHI intensities  $T_{1-T3}$  and  $T_{2-T3}$  are shown in Table 4 together with the maximum and minimum values.

**Table 4.** Daytime and night-time UHI intensities  $T_{1-T3}$  and  $T_{2-T3}$  values for 5 years (i.e., 2014–2018).

Value Discretion	UHI Intensity $T_{1-T3}$ (°C)	Daytime UHI Intensity $T_{1-T3}$ (°C) (6 a.m.–9 p.m.)	Night-time UHI Intensity $T_{1-T3}$ (°C) (9 p.m.–6 a.m.)	UHI Intensity $T_{2-T3}$ (°C)	Daytime UHI Intensity $T_{2-T3}$ (°C) (6 a.m.–9 p.m.)	Night-time UHI Intensity $T_{2-T3}$ (°C) (9 p.m.–6 a.m.)
Maximum value	11.5	11.3	11.5	13.0	11.7	13.0
Minimum value	−12.8	−12.8	−5.4	−13.5	−13.5	−9.9
Average value	1.3	−0.4	4.6	−0.3	−1.1	1.3
Median value	1.7	−0.7	4.6	−0.2	−1.3	1.4

It is worth noting that, considering the period of interest and as summarized in Table 4, the urban and suburban areas of Dubai were in average warmer at night than the rural area by 4.6 °C and 1.3 °C, respectively. On the contrary, during the day, the rural area was in average warmer than the urban and suburban areas (i.e., 0.4 °C and 1.1 °C, respectively).

The frequency distribution of the daytime and night-time values for the UHI intensity  $T_{1-T3}$  and  $T_{2-T3}$  given in (Figure 6) help to understand the distribution of the values representing the UHI intensity during the period of interest.

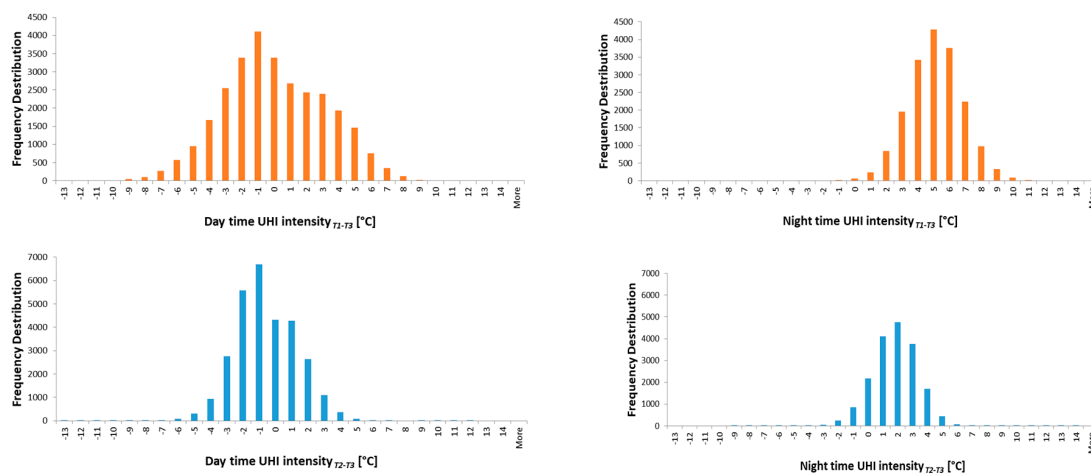
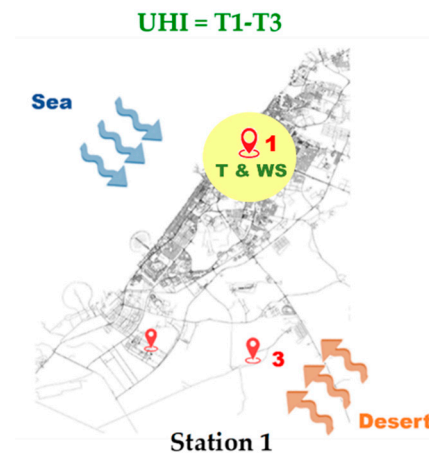


**Figure 6.** Frequency distribution of the daytime and night-time UHI intensity for 5 years (i.e., 2014–2018): daytime UHI intensity  $T_{1-T3}$  (top left), night-time UHI intensity  $T_{1-T3}$  (top right), daytime UHI intensity  $T_{2-T3}$  (bottom left), night-time UHI intensity  $T_{2-T3}$  (bottom right).

Figures 5 and 6 show that the UHI intensity is higher at night than during the daytime in both urban and suburban areas. The urban area presents higher values of average UHI intensity with respect to the suburban area both during the night (i.e., 3.3 °C of difference) and the day (i.e., 0.7 °C of difference).

### 3.3. UHI Intensity $T_{1-T3}$ and Climate Parameters Collected by Station 1

The air temperature and wind speed measured by station 1, located in the Dubai International Airport, were investigated for the six clusters of different ranges of wind direction in relation with the canopy urban heat island intensity (UHI) calculated as the difference between the air temperature measured at the Dubai International Airport (i.e., station 1) and at Saih Al Salem (i.e., station 3), where station 1 is considered as located in an urban area and station 3 is considered as located in a suburban area (Figure 7).



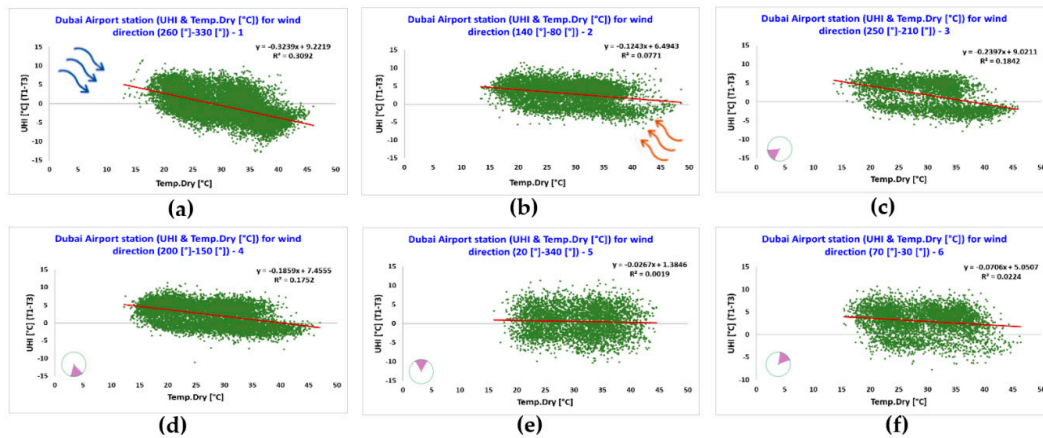
**Figure 7.** Representation of the UHI calculation and the station (i.e., urban station under the yellow circle) selected for the investigation of the climate parameters, i.e., air temperature (T) and wind speed (WS).

Figure 8 shows a comparison of the relation between the hourly canopy UHI intensity (UHI intensity  $T_{1-T3}$ ) and the hourly air temperature measured by station 1 under a different cluster of wind directions. A moderate negative correlation between the temperature and the UHI intensity was found for cluster 1 (i.e., wind direction between  $260^\circ$  and  $330^\circ$  from the seaside) (Figure 8a) where the UHI ranges between  $11.5^\circ\text{C}$  and  $-12.8^\circ\text{C}$ , cluster 3 (i.e., wind direction between  $250^\circ$  and  $210^\circ$  from the coastal area) (Figure 8c) where the UHI ranges between  $10.1^\circ\text{C}$  and  $-7.8^\circ\text{C}$ , and cluster 4 (i.e., wind direction between  $200^\circ$  and  $150^\circ$  from the desert) (Figure 8d) where the UHI ranges between  $11.4^\circ\text{C}$  and  $-11.2^\circ\text{C}$ . The temperature for these three clusters fluctuates between  $47^\circ\text{C}$  and  $12.3^\circ\text{C}$ . A weak negative correlation between the temperature and UHI intensity was found for all the remaining clusters except for cluster 5 (i.e., wind direction located between  $20^\circ$  and  $340^\circ$ ) (Figure 8e) where no correlation was found. The results show that the UHI intensity varies with different wind directions. When the wind is blowing from the desert (i.e., cluster 2) (Figure 8b), the temperature and the UHI are almost independent. Despite the positive impact of the sea breeze, coastal cities suffer from the UHI [41]. Different experimental and numerical investigations have shown the impact of the sea on the development of the UHI in coastal cities [42,43]. The temperature in station 1 is affected by UHI when the wind is blowing from the seaside. It seems that, when there is a sea breeze combined with high temperatures, the negative UHI value is high (Figure 8a). This is due to the fact that the high temperatures recorded by station 1 are mitigated by the sea breeze more than the temperatures recorded by rural station 3, which is closer to the desert and typically reaches higher temperatures during hot days. This pattern is due to advection from the sea breeze cooling mechanism and the flow of air, which is affected by buildings. These results align with those of similar studies in Athens and Sydney [2,7,44,45].

Figure 9 shows a comparison of the relation between canopy UHI intensity (UHI intensity  $T_{1-T3}$ ) and the wind speed measured by station 1 under different clusters of wind directions.

For the wind speed, as for the air temperature, a negative slope of the regression line ( $p$ -value  $< 0.05$ ) is evident in all clusters except in cluster 5 (Figure 9e) where there is no correlation. In this case, the correlation coefficient (R) between the UHI and the wind speed is negative and weak (ranging between  $-0.2$ – $-0.4$  for all clusters) regardless of the wind direction. The results show that the wind speed is lower when the wind blows from the coastal area (i.e., clusters 3 and 6) (Figure 9c,f) with average wind speeds of  $10\text{ km/h}$  and  $11\text{ km/h}$ , respectively. It reaches higher values when the wind blows from the sea (i.e., cluster 1) (Figure 9a) with average wind speeds of about  $18\text{ km/h}$  due to the energy produced by the sea breeze. The results show that wind speed has an impact on the magnitude of the UHI. Results show that the low values of wind speed are more conducive to the development of a UHI [46]. Thus, the data from station 1 shows an inverse relation between the wind speed and UHI

intensity when the wind speed increases for all clusters except cluster 5. This relation is consistent with several studies conducted in various regions [2,47–49]. In cluster 5 (Figure 9e), with the wind from the North, no correlation was found between the wind speed and UHI intensity [2].



**Figure 8.** Comparison between the UHI and the temperature relation under different clusters of wind directions: (a) cluster 1, (b) cluster 2, (c) cluster 3, (d) cluster 4, (e) cluster 5, and (f) cluster 6.

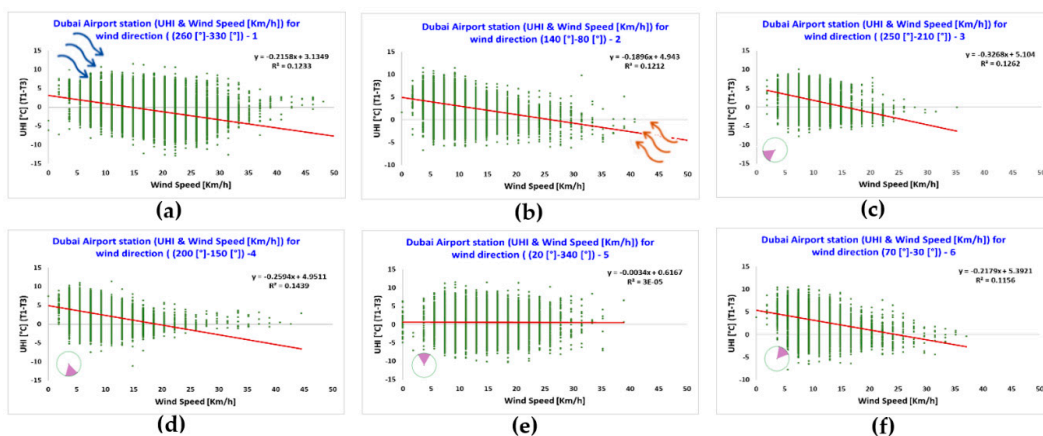


**Figure 9.** Comparison between the UHI and the wind speed relation under different clusters of wind directions: (a) cluster 1, (b) cluster 2, (c) cluster 3, (d) cluster 4, (e) cluster 5, and (f) cluster 6.

### 3.4. UHI Intensity $T_{1-T3}$ and Climate Parameters Collected by Station 2

The air temperature and wind speed measured by station 2 were investigated for the six clusters of wind direction in relation to the UHI calculated as in the previous section and as shown in Figure 10.

A strong negative correlation between the air temperature measured by station 2 and (UHI intensity  $T_{1-T3}$ ) was found for cluster 1 (Figure 11a) and cluster 3 (Figure 11c), where the UHI values range from 10.7 °C to −12.8 °C and the temperatures range between 48.2 °C and 12.4 °C for both clusters. The values of the correlation coefficient comprise about 40% of the data. Regarding the other clusters, there is a weak and negative linear UHI & relation between the temperature and the UHI intensity as shown in Figure 11.

As evident in Figure 12, the canopy UHI intensity has a moderate negative correlation with wind speed, averaging around 14 km/h, in cluster 5 (Figure 12e) where the wind comes from the seaside direction. The other clusters in the same station show a weak and negative correlation with close (R) values varying between −0.2 and −0.5. The results indicate that the high values of wind speed decrease the differences in the temperatures for all clusters, as observed in the study of Sydney [2] as well as in [50]. Additionally, the impact on UHI intensity in terms of all wind directions is minimized due to the effects of the two parameters. An increase in wind speed in the urban area enhances the heat flux, whose heating impact on the urban environment is stronger than the enhanced cooling

effect [49,51]. It could also be that an urban atmosphere can absorb the heat from solar radiation during the daytime. These outcomes are supported by the results of previous studies [52,53]. As shown, the station recorded a maximum ambient temperature of 48.5 °C in July 2015, while the reference station recorded 50.2 °C for the same year.

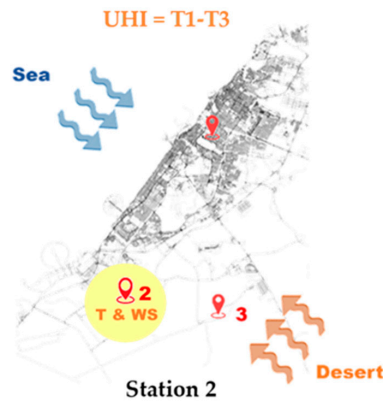


**Figure 10.** Representation of the UHI calculation and the station (i.e., the suburban station under the yellow circle) selected for the investigation of the climate parameters, i.e., air temperature (T) and wind speed (WS).

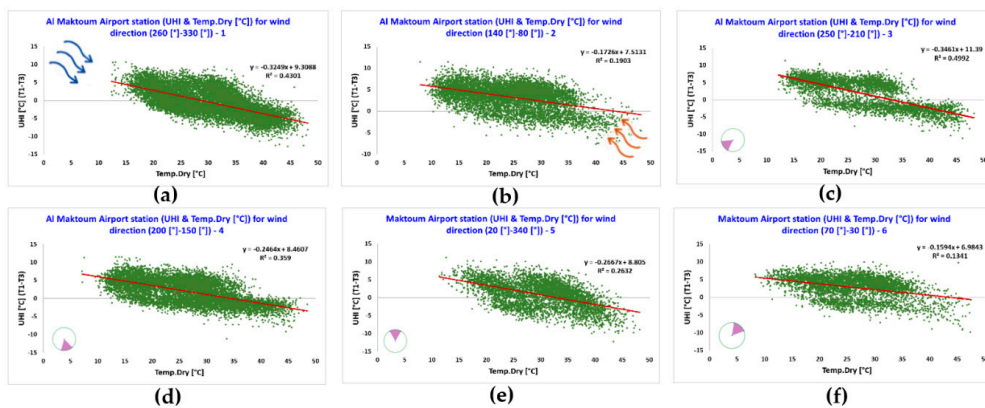


**Figure 11.** Comparison between the UHI and the temperature relation under different clusters of wind directions: (a) cluster 1, (b) cluster 2, (c) cluster 3, (d) cluster 4, (e) cluster 5, and (f) cluster 6.

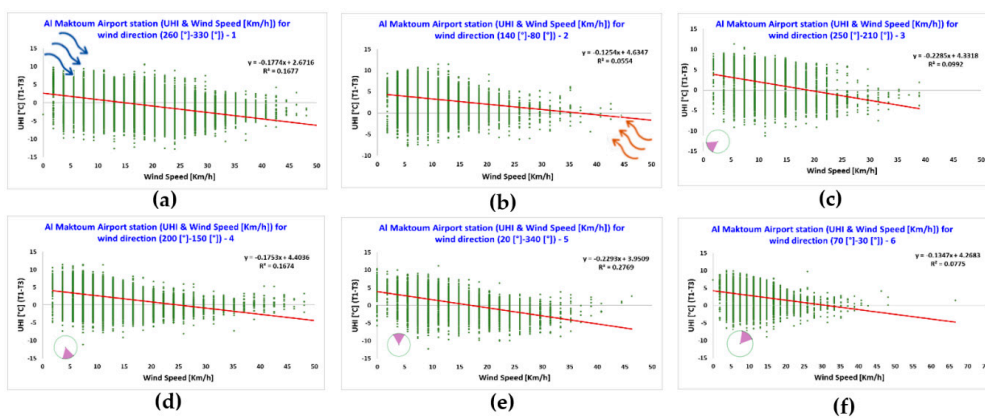


**Figure 12.** Comparison between the UHI and the wind speed relation under different clusters of wind directions: (a) cluster 1, (b) cluster 2, (c) cluster 3, (d) cluster 4, (e) cluster 5, and (f) cluster 6.

### 3.5. UHI Intensity $T_2-T_3$ and Climate Parameters Collected by Station 1

The air temperature and wind speed measured by station 1 were investigated for the six clusters of different ranges of wind direction in relation with the canopy urban heat island intensity (UHI) calculated as the difference between the air temperature measured at the Al Maktoum International Airport (i.e., station 2) and at Saih Al Salem (i.e., station 3) (Figure 13).

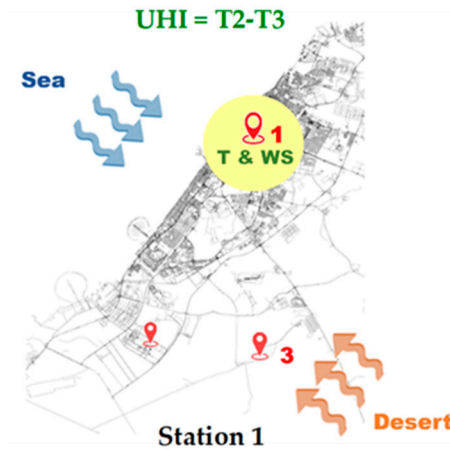


**Figure 13.** Representation of the UHI calculation and the station (i.e., the urban station under the yellow circle) selected for the investigation of the climate parameters, i.e., air temperature (T) and wind speed (WS).

Figure 14 shows a moderate negative linear relation between the temperature and the (UHI intensity  $T_2-T_3$ ) for cluster 1 (Figure 14a). The temperature for this cluster ranges between 46.1 °C and 13 °C with an average value close to 30.8 °C and the UHI ranges from 12.4 °C to −13.5 °C. For the five other clusters, the canopy UHI intensity shows a weak negative correlation with temperature, with few variations. Here, the synoptic climate conditions associated with the advection and convection phenomena play a role in this mechanism as does the additional anthropogenic heat in the area. These findings are supported by several other studies [2,7,54,55]. Other previous studies have reported that the daytime intensity of the heat island is reduced under specific synoptic conditions [56,57].

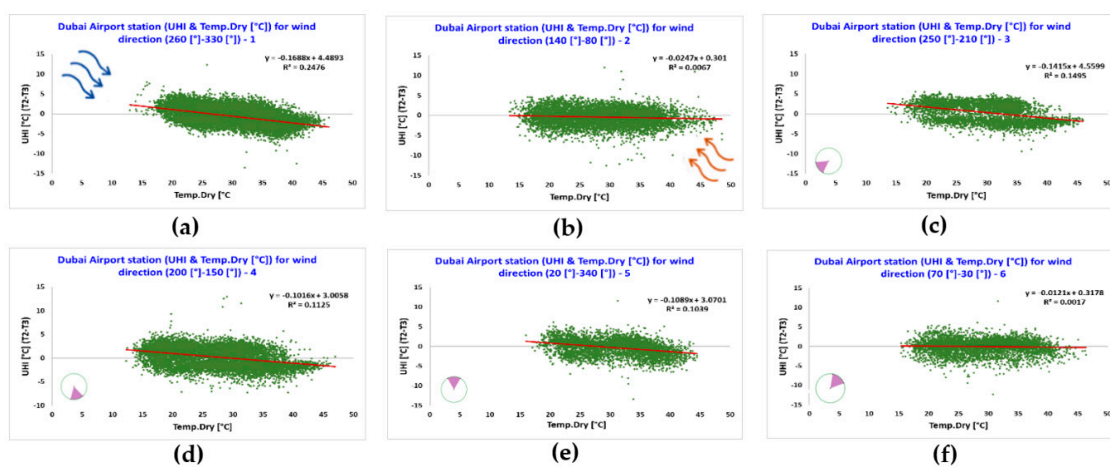


**Figure 14.** Comparison between the UHI and the temperature relation under different clusters of wind directions: (a) cluster 1, (b) cluster 2, (c) cluster 3, (d) cluster 4, (e) cluster 5, and (f) cluster 6.

In Figure 15, the (UHI intensity  $T_2-T_3$ ) ranges between 11.6 °C and −13.4 °C showing a moderate negative correlation when the wind speed ranges from 39 km/h to 0 km/h, with an average value close

to 15 km/h when the wind is coming from the North as in cluster 5 (Figure 15e). The data of the cluster demonstrate a 22.8% variation in the UHI intensity compared with the other clusters which have a very weak correlation with the UHI intensity as they are close to zero. Moreover, in regard to western and north-western wind directions, there is a negative relation between the UHI and both the temperature and wind speed, similar to the findings of other studies [2].

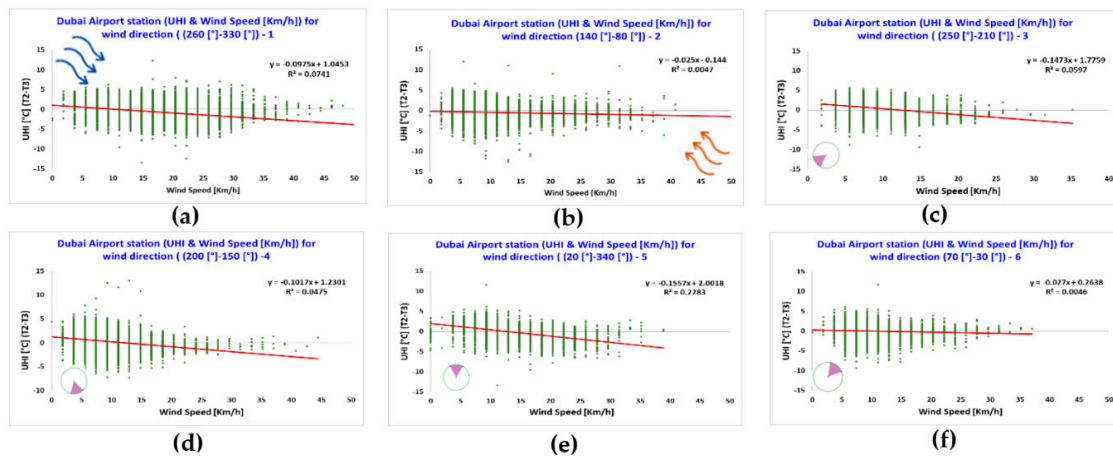


**Figure 15.** Comparison between the UHI and the wind speed relation under different clusters of wind directions: (a) cluster 1, (b) cluster 2, (c) cluster 3, (d) cluster 4, (e) cluster 5, and (f) cluster 6.

### 3.6. UHI Intensity $T_2-T_3$ and Climate Parameters Collected by Station 2

The air temperature and wind speed measured by station 2 were investigated for the six clusters of wind direction in relation to the UHI calculated as described in the previous section and as shown in Figure 16.

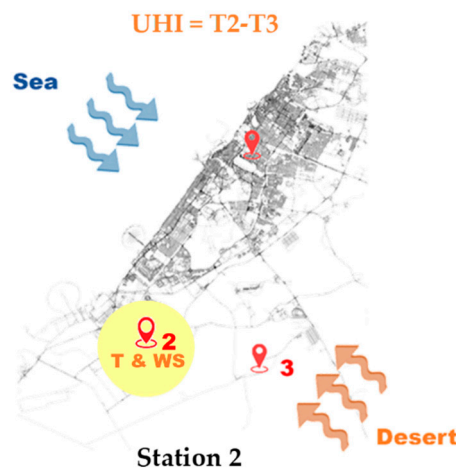


**Figure 16.** Representation of the UHI calculation and the station (i.e., the suburban station under the yellow circle) selected for the investigation of the climate parameters, i.e., air temperature (T) and wind speed (WS).

Cluster 1 (Figure 17a) and cluster 3 (Figure 17c) show a moderate negative correlation between the temperature and (UHI intensity  $T_2-T_3$ ). The temperature in both clusters ranges between 48.2 °C and 12.2 °C. However, in the other clusters, there is a negative weak correlation between the temperature and the UHI intensity, as shown in Figure 17.

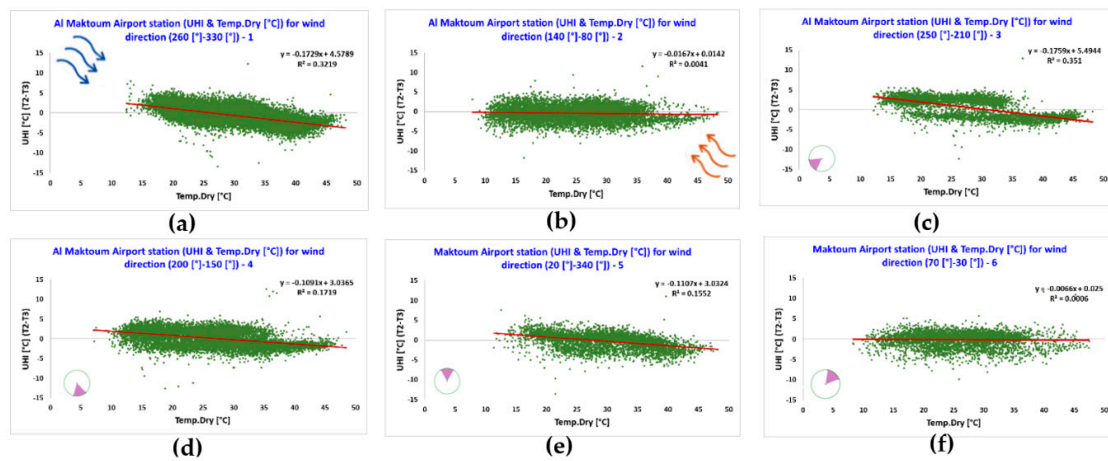


**Figure 17.** Comparison between the UHI and the temperature relation under different clusters of wind directions: (a) cluster 1, (b) cluster 2, (c) cluster 3, (d) cluster 4, (e) cluster 5, and (f) cluster 6.

Figure 18 shows a weak negative correlation which means little relation between the wind speed and UHI intensity; it is close to zero in all clusters [2] for Al Maktoum International Airport (station 2). The results show no significant difference between station 1 and station 2 regarding the climate parameters and the UHI intensity phenomenon. In the surrounding area of station 1, the prevailing wind is coming from the sea. It is clear that when the wind is coming from the seaside or the desert, due to the higher energy embedded in the synoptic conditions, the wind speed will be higher than when the wind direction is parallel to the coast (cluster 3) (Figure 18c) These conclusions are supported by previous studies undertaken in Asian and Australian cities [2,40,49,58].

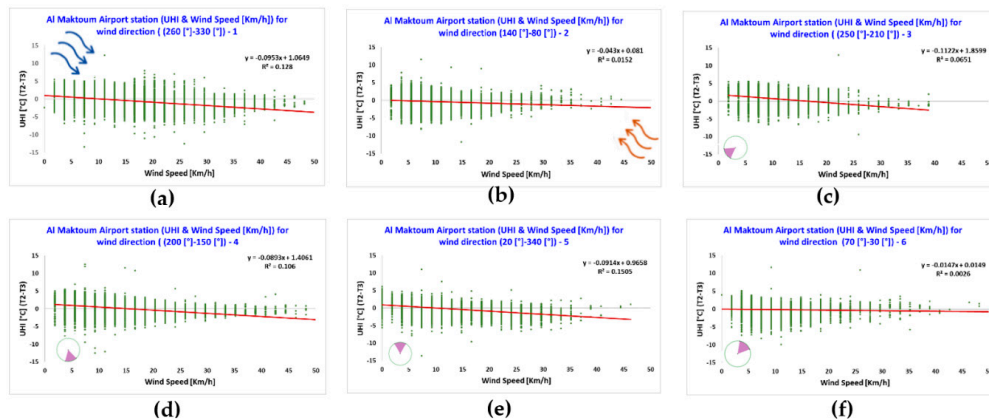


**Figure 18.** Comparison between the UHI and the wind speed relation under different cluster of wind directions: (a) cluster 1, (b) cluster 2, (c) cluster 3, (d) cluster 4, (e) cluster 5, and (f) cluster 6.

### 3.7. UHI Intensity $T_{1-T3}$ and Climate Parameters Collected by Station 3

As done previously with both stations 1 and 2, the same procedure was followed to determine the temperature and wind speed for Saih Al Salem (i.e., station 3) and their relation with the UHI magnitude, calculated as the difference between the temperature measured at the Dubai International Airport (i.e., station 1) and at the Saih Al Salem area for all clusters of wind direction (Figure 19).

Figure 20 shows that for all clusters, there is a strong negative correlation between the UHI intensity  $T_{1-T3}$ , ranging from 11.5 °C to −12.8 °C, and the air temperature, fluctuating between 50.8 °C and 4.7 °C, with an average of 28.3 °C. To recap, cluster 1 (Figure 20a) is from the sea direction, cluster 2 (Figure 20b) from the desert area, and cluster 3 (Figure 20c) from the coastal area. In terms of this parameter, there is a variation from 55% to 65% in UHI intensity among these three clusters. When the temperature increases, so does the intensity of the UHI.

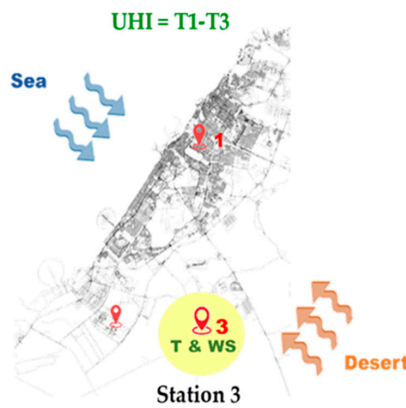


**Figure 19.** Representation of the UHI calculation and the station (i.e., the rural station under the yellow circle) selected for the investigation of the climate parameters, i.e., air temperature (T) and wind speed (WS).

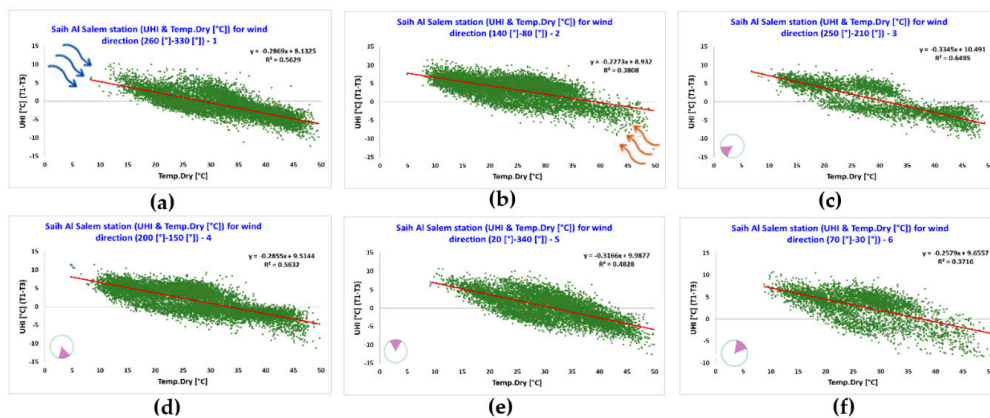


**Figure 20.** Comparison between the UHI and the temperature relation under different clusters of wind directions: (a) cluster 1, (b) cluster 2, (c) cluster 3, (d) cluster 4, (e) cluster 5, and (f) cluster 6.

The slope of the regression line ( $p$  value < 0.05) shown in Figure 21 indicates that for all clusters, there is a moderate negative relation between the wind speed and the UHI intensity. For all six clusters, the results indicate a relation ranging from moderate to strong between the UHI intensity and the two climate parameters in Saih Al Salem station. Synoptic weather conditions could have an impact on the parameter mechanisms as could the open desert space criterion. Numerous previous studies have reported the same results [2,47,54].

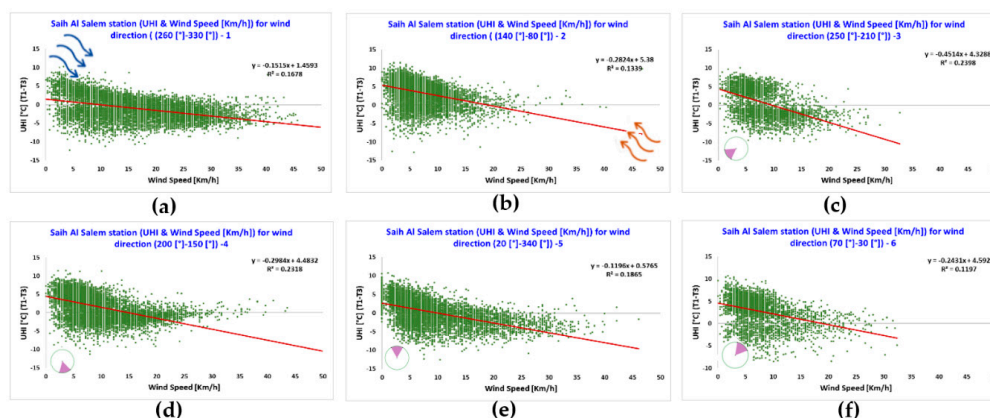


**Figure 21.** Comparison between the UHI and the wind speed relation under different clusters of wind directions: (a) cluster 1, (b) cluster 2, (c) cluster 3, (d) cluster 4, (e) cluster 5, and (f) cluster 6.

### 3.8. UHI Intensity $T_2-T_3$ and Climate Parameters Collected by Station 3

The temperature and wind speed measured by station 3 were investigated for the six clusters of wind direction as in the previous sections. The UHI was calculated as the difference between the temperature measured by station 2 (i.e., Al Maktoum International Airport) and station 3 (i.e., Saih Al Salem) as shown in Figure 22.

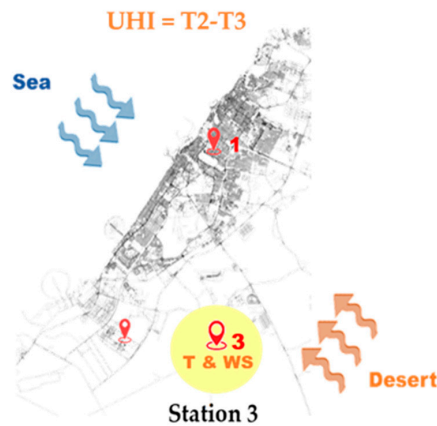


**Figure 22.** Representation of the UHI calculation and the station (i.e., the urban station under the yellow circle) selected for the investigation of the climate parameters, i.e., air temperature (T) and wind speed (WS).

The scatter plots in Figure 23 show strong negative correlations for the different clusters between the UHI intensity  $T_2-T_3$  and the temperature in cluster 1 (Figure 23a) from the sea direction, cluster 3 (Figure 23c) from the coastal area, cluster 4 (Figure 23d) from the desert side, and cluster 5 (Figure 23e) from the sea. The data demonstrates about 47%, 57%, 41%, and 37% variation in the canopy UHI, respectively. For the other two clusters, there is a weak and negative linear association between the temperature and UHI intensity; also, the temperature had independent effects on UHI intensity [2,7,55,59].

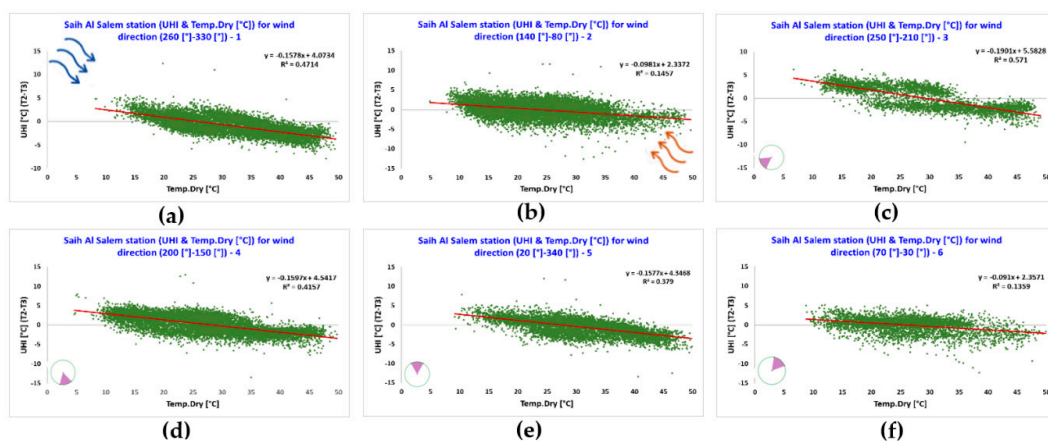


**Figure 23.** Comparison between the UHI and the temperature relation under different clusters of wind directions: (a) cluster 1, (b) cluster 2, (c) cluster 3, (d) cluster 4, (e) cluster 5, and (f) cluster 6.

As shown in Figure 24, the slope of the regression line ( $p$  value  $< 0.05$ ) indicates a moderate negative correlation between the wind speed and the canopy UHI magnitude in cluster 3 (Figure 24c), cluster 4 (Figure 24d) and cluster 5 (Figure 24e). The UHI intensity for these three clusters is between 13 °C and -13.5 °C, while the wind speed ranges from 51 km/h to 0 km/h, with an average value close to 9 km/h. The results indicate moderate to strong relations between the UHI magnitude and the two

climate parameters for this station. These results may be due to the presence of different synoptic weather systems of heating mechanism, a desert wind with a cooling mechanism, and coastal wind, which are created by the combination of climate parameters. These conclusions are compatible with those of previous studies conducted in various regions [2,47,55].

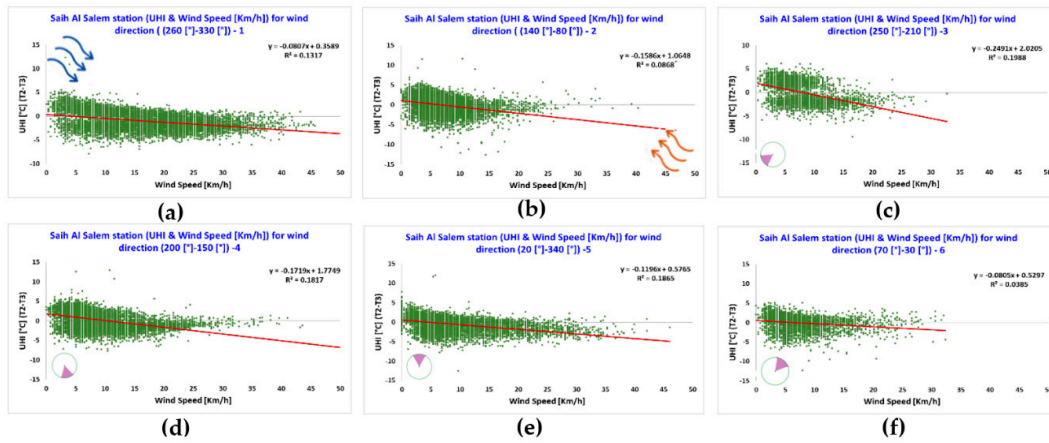


**Figure 24.** Comparison between the UHI and the wind speed relation under different cluster of wind directions: (a) cluster 1, (b) cluster 2, (c) cluster 3, (d) cluster 4, (e) cluster 5, and (f) cluster 6.

### 3.9. Correlation between UHI Intensity $T_{1-T3}$ and $T_{2-T3}$ and Climate Parameters

Figure 25 shows a comparison between the UHI intensity  $T_{1-T3}$  and UHI intensity  $T_{2-T3}$  and the hourly air temperature measured by station 1 and station 2 under the respective clusters of wind directions.

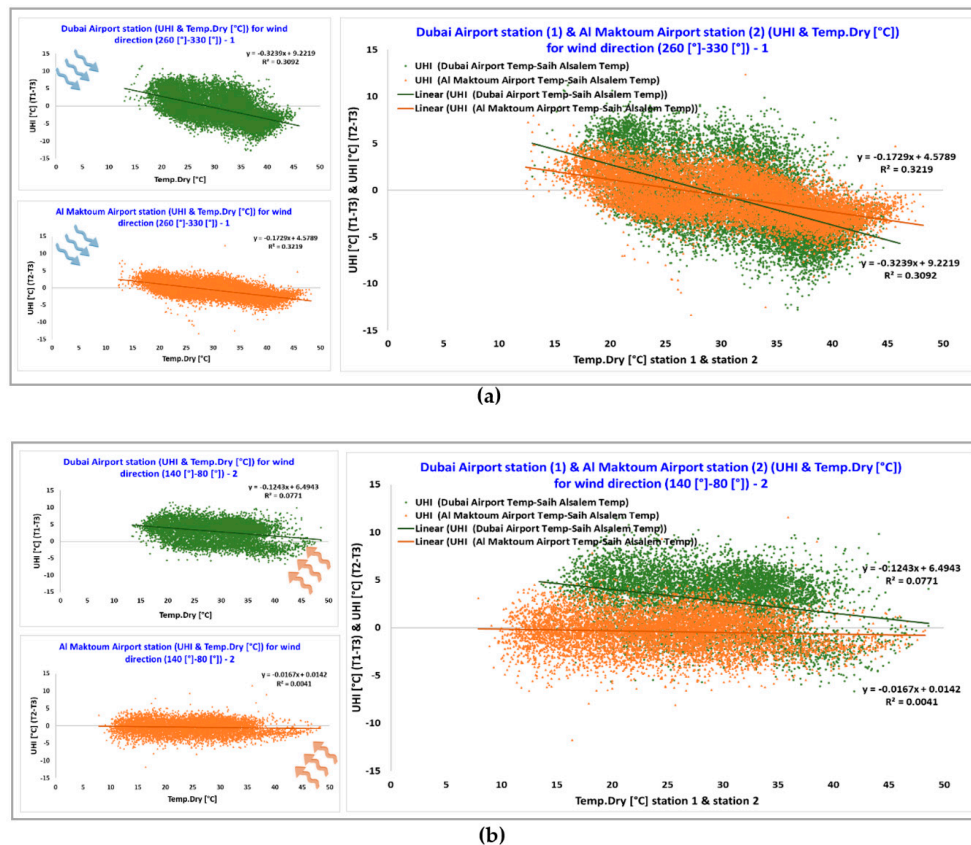
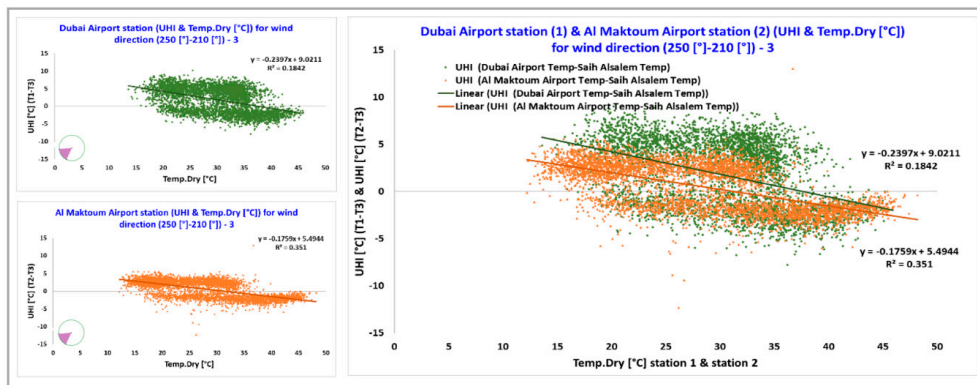
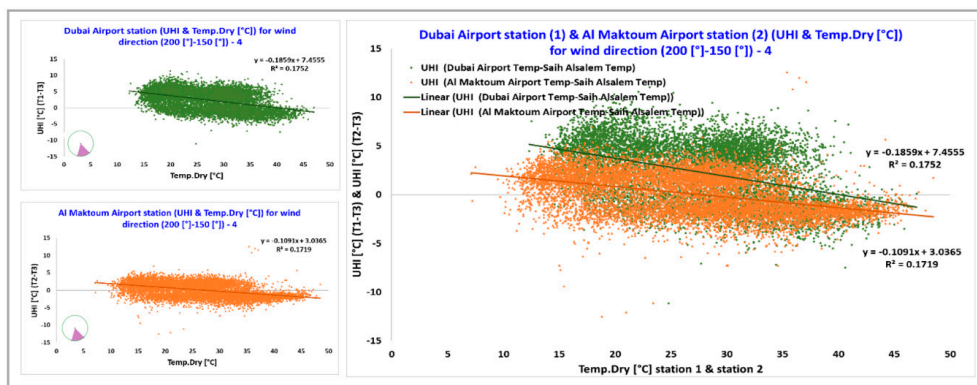


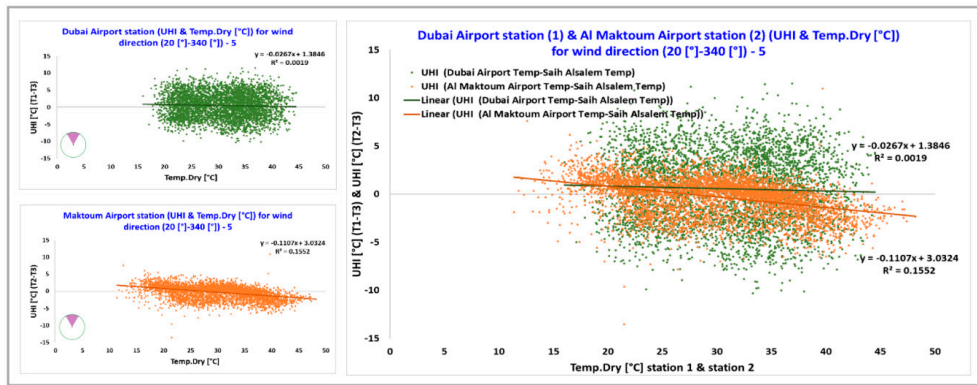
**Figure 25.** Cont.



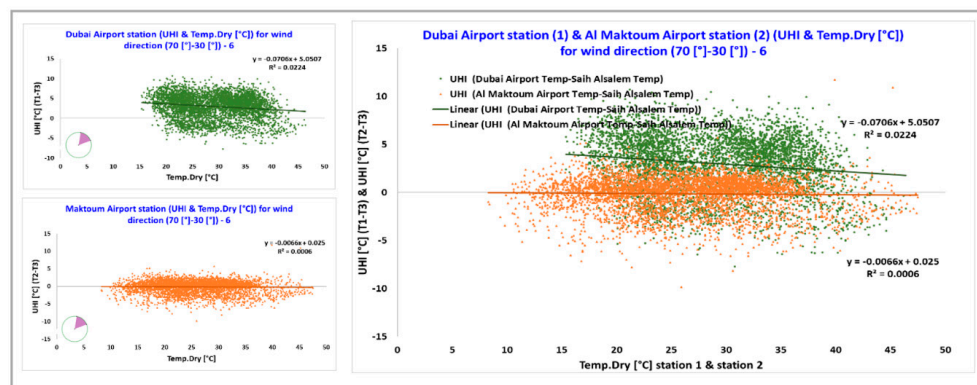
(c)



(d)



(e)



(f)

**Figure 25.** Comparison between the UHI and the air temperature relation measured in the urban (green) and suburban (orange) areas under different clusters of wind directions: (a) cluster 1, (b) cluster 2, (c) cluster 3, (d) cluster 4, (e) cluster 5, and (f) cluster 6.

A strong and negative correlation coefficient (R) between the temperature and UHI intensity  $T_{1-T3}$  and  $T_{2-T3}$  was found in Al Maktoum International Airport when the wind was coming from the sea. Hence, the temperature only demonstrates about 32% variation in the urban heat island intensity. Whereas, when the wind is coming from the desert side (cluster 2) (Figure 25b), there is no correlation between the temperature and the intensity of UHI at station 2 (i.e., Al Maktoum International Airport), which is close to zero. These results are aligned with those of other studies conducted in different regions [2,49,58].

Figure 26 compares the correlations between the wind speed and the canopy UHI intensity for both stations through the same procedure used for measuring the parameters of temperature and UHI intensity.

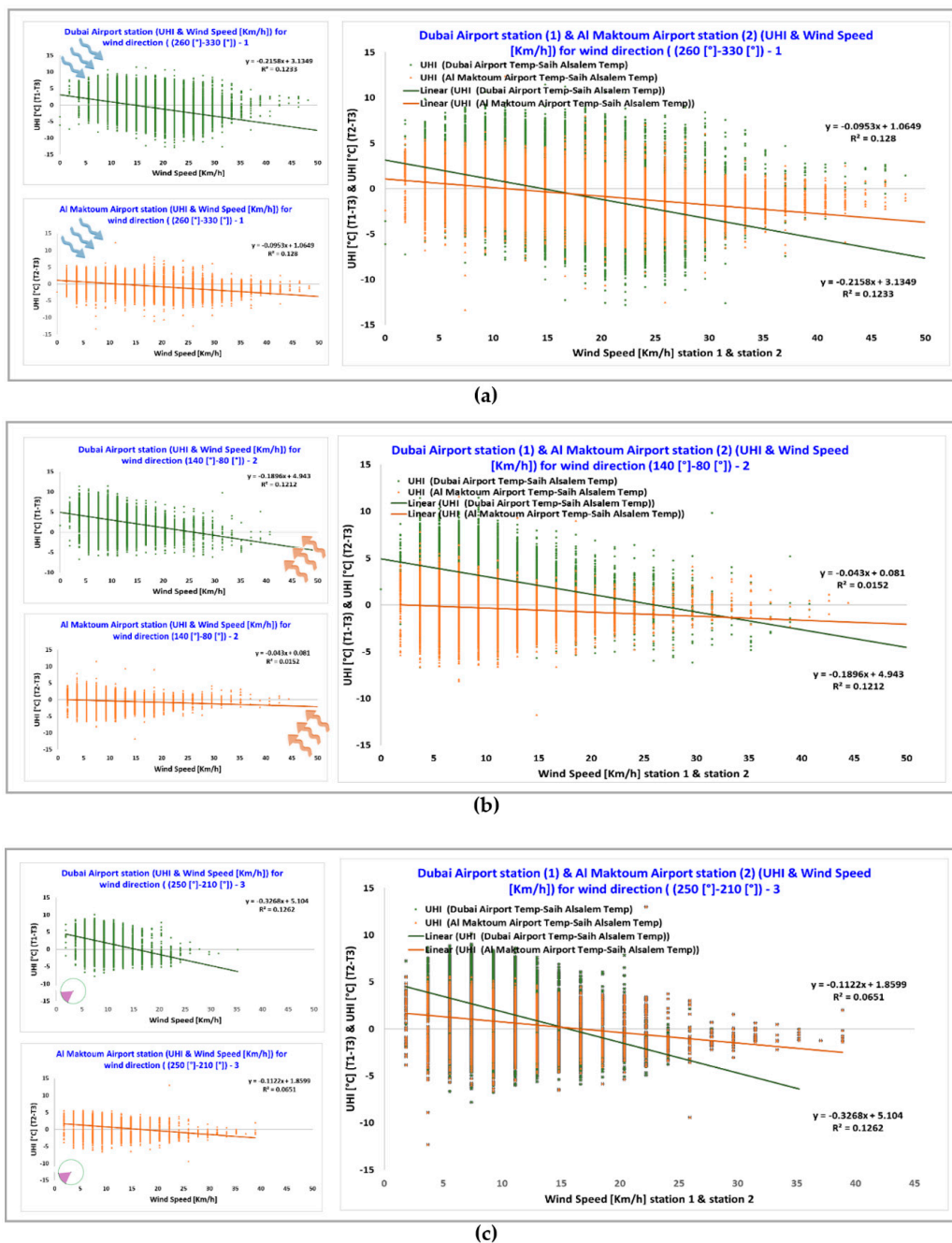
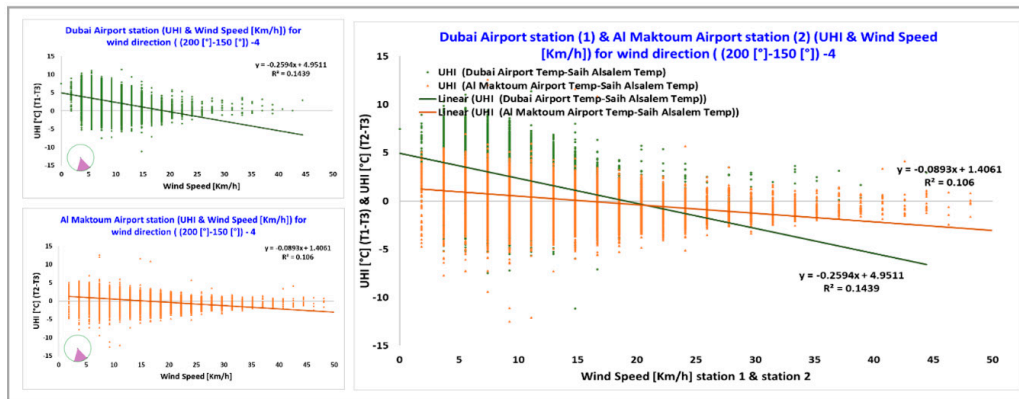
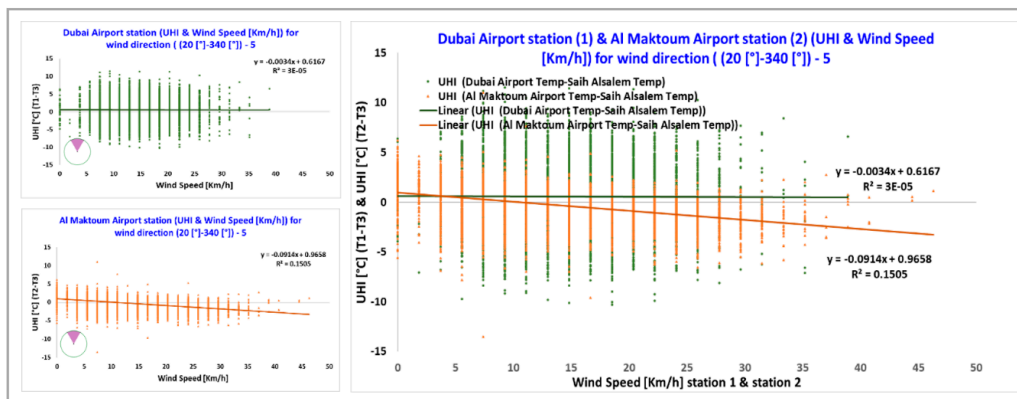


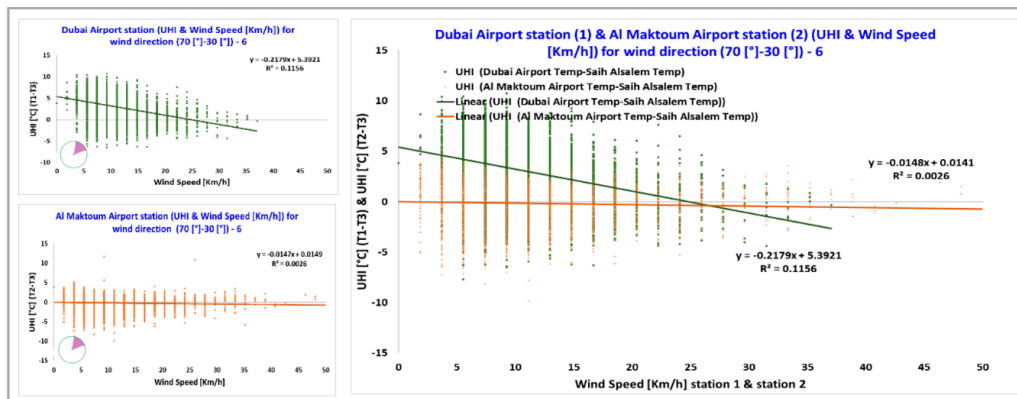
Figure 26. Cont.



(d)



(e)



(f)

**Figure 26.** Comparison between the UHI and the wind speed relation measured in the urban (green) and suburban (orange) areas under different clusters of wind directions: (a) cluster 1, (b) cluster 2, (c) cluster 3, (d) cluster 4, (e) cluster 5, and (f) cluster 6.

Results show that when the wind direction is coming from the sea, there is a weak negative correlation between the wind speed and the UHI intensity. For cluster 1 (Figure 26a), the wind speed is responsible for only a 12% variation in the UHI magnitude. However, when the wind is coming from the desert side as in cluster 2 (Figure 26b), there is no correlation between the wind speed UHI intensity. These results are supported by those of other studies [2].

#### 4. Discussion

Urban areas are facing several climate issues, one of which is the urban heat island (UHI) phenomenon. Thus, to understand the characteristics of UHI and its effects on the built environment,

this study investigated the correlation between the canopy UHI and two meteorological parameters, air temperature and wind speed, with given specific ranges of wind direction. This was done by collecting and analyzing the hourly data from three meteorological stations situated in different areas of Dubai (i.e., urban, suburban, and rural areas).

It has been observed that the UHI intensity is larger at night in both urban and suburban areas and that the urban area presents the highest values of average UHI intensity. The main reason for the negative UHI at night is the presence of the heat that, given the intense incident solar radiation, remains trapped in the urban and suburban areas according to the geometry and density of the built environment and the thermal-optical properties of the urban surfaces. During the day, the built areas in Dubai act as urban cool islands showing negative UHI intensity values.

The analysis results show that canopy UHI intensity varies with wind direction and meteorological conditions. This has been confirmed by other studies carried out in cities with different climatic conditions [60,61]. Moreover, in regard to UHI intensity  $T_{1-T3}$ , the data from the urban meteorological station indicated that air temperature and UHI were almost independent when the wind was coming from the desert (i.e., from the East and South-East), while the temperature is affected by UHI when the wind is flowing from the sea (i.e., West and North-West) thanks to the cooling mechanism of the sea breeze and the short distance of the seashore to the station 1 [41,43]. It could also be influenced by the building's orientation. These results are consistent with the findings of studies conducted in Sydney where the eastern suburbs benefited from the significant cooling mechanism of the sea breeze and the variations in UHI were a function of the prevailing climate conditions [2]. Moreover, it appears that a negative UHI intensity exists during the day and the night (i.e., the temperature in the urban area is lower than the temperature in the rural area), which is also observed in many cities. Several factors could be the cause of negative UHI values. In this case, two of the main reasons could be the hot air that, coming from the desert, increases the air temperature in the rural area more than in the urban area and the presence of the sea breeze [9,10] mitigates the urban overheating when the cold wind blows from the seaside. This confirms the many experimental investigations about the effect of the sea breeze on the magnitude of the UHI [43]. In addition, several studies have demonstrated that the flow of the sea breeze across the city is delayed by the UHI because there is a stagnation zone over the built environments [45,62]; other studies conclude that UHI could accelerate the front of the wind blowing from the seaside and moving across a city, more than in rural areas where it has little or no effect [63,64].

The results of this study, which focuses on wind speed, proved that wind speed has an impact on the magnitude of UHI [58] depending on the prevailing climatic conditions and the wind direction. Similar to the study of Sydney in 2017, a relation between the wind speed and UHI intensity was identified in this study [2]. Moreover, other studies in Chicago, Salamanca, and Granada explain the impact of UHI under ambient climatic conditions such as cloud cover and wind [50,65,66].

Regarding the cloud cover, it was observed that the night-time UHI intensity in the urban and suburban areas reaches the highest values in the presence of clear sky days, due to the larger amount of heat that is absorbed by the built area during the day and then released at night.

In the urban station (i.e., station 1), a reverse correlation between the wind speed and UHI was observed. For most wind directions, when the wind speed increased, the UHI decreased. However, when the wind is coming from the North, the correlation is close to zero. These results are consistent with the findings of previous studies that have examined the impact of wind speed on UHI magnitude in various areas such as Ibadan and Ulaanbaatar [3,47,48].

Moreover, a significantly strong and negative correlation was observed in the suburban area (i.e., station 2) between the levels of the air temperature and wind speed and the magnitude of the UHI. It was found that the effect of UHI intensity in all wind directions is decreasing or even minimized with the increase in the temperature and especially of the wind speed. A possible explanation is that when the wind speed increases, the temperature variations (i.e., between 48.6 °C and 12.3 °C with an average value of about 29.5 °C) gradually decrease since higher wind speeds are connected with

the advection of air masses that tend to minimize the temperature differences. This relation has been observed in several cities around the world [51,67], as well as in the urban station (i.e., station 1).

It was observed that when the wind speed is low or zero, the UHI has a positive value because the temperature in the urban area (where the urban surface easily absorbs solar radiation) is higher than in the rural area (where the natural surface has less absorption). When the wind speed is very high, the UHI effect disappears due to the heat dissipation produced by the wind. Similarly, the study of Athens found that the high temperatures resulted from solar radiation when the wind speed was low [52].

The data collected by reference station 3 (i.e., Saih Al Salem), which is located in a rural desert village far from the seacoast, show a moderate to a strong correlation between the UHI and the temperature and wind speed, for all wind directions. This is similar to the relation found in the studies of Ibadan and Sydney [2,47].

In the case of UHI intensity  $T_2-T_3$ , the UHI magnitude varies between 11.5 °C and −12.8 °C. It is found that the results for the urban station are similar to those observed in the suburban station through the correlation methodology used for the UHI magnitude and the climate parameters. It was also observed that there were no significant differences between the two stations during the 5 year period of interest. This indicates that when the wind comes from the sea (i.e., western and north-western) directions, there is a moderate negative relation between the UHI and both the temperature and wind speed. The negative results could be due to the additional anthropogenic heat and the cooling rates caused by evaporation. Data analysis showed an inverse relation between the wind speed and the UHI intensity where when the former increased, the latter decreased. In contrast, for all other wind directions, the analysis indicated no correlation between the UHI intensity and both temperature and wind speed. These results are aligned with those of previous studies conducted in Asian and Australian cities [58].

The results show that, in the case of station 3, there is a significant correlation between the meteorological parameters and UHI. A moderate to a quite strong relation is found between this UHI magnitude and the two parameters (i.e., temperature and wind speed) for all the wind directions compared to the previous case of the UHI intensity  $T_1-T_3$ . These results could occur with synoptic weather and specific conditions created by the combination of climate parameters, which is consistent with the findings from the previous studies carried out in various regions [2,47].

The results of this study indicate that wind speed and temperature have an impact on the urban heat island depending on the prevailing weather conditions on whether the wind comes from the sea or from the desert. However, the urban area is the one most affected. In fact, the relations, found in this study, between the meteorological parameters and UHI, have several implications for future urban planning. Strategies are needed to reduce the temperatures and have better cooling systems within urban areas in order to control urban heat islands. There is a need to establish guidelines for urban planning and design so that urbanization is sustainable. Worth noting is the fact that one of the challenges faced in this study was the limited availability of meteorological parameters and adequate monitoring data covering a greater number of years.

## 5. Conclusions

The aim of this paper was to examine the correlation between the intensity of the canopy urban heat island and the various meteorological parameters (e.g., temperature, wind speed, and wind direction) when the wind is coming from different directions such as from the seaside and the desert side. Hourly data of climate parameters were derived from five years (2014–2018) of monitoring from three meteorological stations located in an urban, suburban, and a rural area of Dubai. Six clusters of wind directions were identified to perform a cluster analysis on the available set of climatic data.

It was found that the temperature and wind speed results differed between the western (seaside) and eastern (desert side) parts of Dubai. The UHI intensity varies with the wind direction and meteorological conditions. Regarding the UHI intensity  $T_1-T_3$ , it was found that when the wind in

the urban area was coming from the desert, the temperature and the UHI were almost independent. However, a relation exists when the wind is coming from the seaside (i.e., sea breeze). Therefore, the wind speed influences the UHI intensity depending on the synoptic climate conditions and wind directions. A reverse correlation was found between the wind speed and UHI intensity for all wind directions, except the North direction where no correlation was found in the urban area. In the suburban area, an inverse relation was observed between the wind speed and the magnitude of UHI, for all wind directions. At the same time, a moderate to strong correlation was found between the UHI and both temperature and wind speed for all wind directions in the rural area.

In contrast, in the case of the UHI intensity  $T_2-T_3$ , it was observed that in the urban and suburban areas, there was a similar correlation between the UHI and the climate parameters when the wind was blowing inland from the sea due to additional anthropogenic heat and evaporation. No correlation was observed for all other wind directions. A moderate to a strong association was found between the UHI and the two climate parameters for all the wind directions in the open zone of the desert, where the reference station (i.e., rural area) is located, due to a combination of climate parameters and synoptic conditions.

From that perspective, the wind that flows from the seaside or the desert side is completely different as the air coming from the sea is cooler, which decreases the temperature and minimizes the UHI. Thus, an onshore wind cools the air temperature of the area depending on the wind speed; hence, the higher the wind speed, the lower will be the magnitude of the UHI. On the other hand, the wind coming from the desert is warmer, producing dry hot weather conditions and increasing the temperature. However, occasionally the wind blowing from the desert has different effects on temperature depending on other factors.

This study, investigating the canopy UHI phenomenon in the coastal and desert areas of Dubai, contributes to a deeper understanding of the local microclimate and urban overheating in desert regions that is essential to inform the climate-resilient urban design and planning. It was observed that the sea breeze plays a vital role in the urban zone and the seashore area, contributing to the mitigation of the summer urban and suburban warming. The results of this study confirmed that additional mitigation strategies for heat reduction should be implemented in desert cities to reduce the thermal stress in the urban ecosystem and avoid many issues that can be caused by high urban temperatures such as heat-related illness and mortality and uncomfortable outside areas.

Further studies should be performed to better understand the overall UHI phenomenon in Dubai, for example also investigating the surface UHI and the boundary UHI with the aim to cover different scales of investigation.

**Author Contributions:** Conceptualization, G.P. and M.S.; methodology, M.S.; formal analysis, A.M.; investigation, A.M., G.P. and M.S.; resources, E.T.; data curation, A.M. and G.P.; writing—original draft preparation, A.M. and G.P.; writing—review and editing, A.M., G.P., E.T. and M.S.; visualization, A.M. and G.P.; supervision, G.P. and M.S. All authors have read and agreed to the published version of the manuscript.

**Funding:** This research received no external funding.

**Acknowledgments:** The authors express their gratefulness to the UAE National Center of Meteorology (NCM) for providing the data used in this study.

**Conflicts of Interest:** The authors declare no conflict of interest.

## References

1. Un.org. World's Population Increasingly Urban with More Than Half Living in Urban Areas. Available online: <https://www.un.org/en/development/desa/news/population/world-urbanization-prospects-2014.html#:~:text=The%202014%20revision%20of%20the,population%20between%202014%20and%202050> (accessed on 6 June 2020).
2. Santamouris, M.; Haddad, S.; Fiorito, F.; Osmond, P.; Ding, L.; Prasad, D.; Zhai, X.; Wang, R. Urban Heat Island and Overheating Characteristics in Sydney, Australia. An Analysis of Multiyear Measurements. *Sustainability* **2017**, *9*, 712. [CrossRef]

3. Oke, T.R. The energetic basis of the urban heat island. *Q. J. R. Meteorol. Soc.* **1982**, *108*, 1–24. [[CrossRef](#)]
4. Oke, T.R.; Johnson, G.T.; Steyn, D.G.; Watson, I.D. Simulation of surface urban heat islands under ‘ideal’ conditions at night part 2: Diagnosis of causation. *Bound. Layer Meteorol.* **1991**, *56*, 339–358. [[CrossRef](#)]
5. Santamouris, M. Recent progress on urban overheating and heat island research. Integrated assessment of the energy, environmental, vulnerability and health impact. Synergies with the global climate change. *Energy Build.* **2020**, *207*, 109482. [[CrossRef](#)]
6. Santamouris, M. Cooling the cities—A review of reflective and green roof mitigation technologies to fight heat island and improve comfort in urban environments. *Sol. Energy* **2014**, *103*, 682–703. [[CrossRef](#)]
7. Santamouris, M.; Paolini, R.; Haddad, S.; Synnefa, A.; Garshasbi, S.; Hatvani-Kovacs, G.; Gobakis, K.; Yenneti, K.; Vasilakopoulou, K.; Feng, J.; et al. Heat mitigation technologies can improve sustainability in cities. An holistic experimental and numerical impact assessment of urban overheating and related heat mitigation strategies on energy consumption, indoor comfort, vulnerability and heat-related mortality and morbidity in cities. *Energy Build.* **2020**, *217*, 110002. [[CrossRef](#)]
8. Santamouris, M.; Kolokotsa, D. *Urban Climate Mitigation Techniques*; Routledge: London, UK, 2016.
9. Sasaki, Y.; Matsuo, K.; Yokoyama, M.; Sasaki, M.; Tanaka, T.; Sadohara, S. Sea breeze effect mapping for mitigating summer urban warming: For making urban environmental climate map of Yokohama and its surrounding area. *Urban Clim.* **2018**, *24*, 529–550. [[CrossRef](#)]
10. Kawamoto, Y.; Yoshikado, H.; Ooka, R.; Hayami, H.; Huang, H.; Khiem, M.V. Sea Breeze Blowing into Urban Areas: Mitigation of the Urban Heat Island Phenomenon. In *Ventilating Cities: Air-flow Criteria for Healthy and Comfortable Urban Living*; Springer: Dordrecht, The Netherlands, 2012; pp. 11–32. [[CrossRef](#)]
11. Comstock, M.; Garrigan, C.; Pouffary, S.; Feraudy, T.d.; Halcomb, J.; Hartke, J.J.U.N.E.P. *Building Design and Construction: Forging Resource Efficiency and Sustainable Development*; United National Environmental Program (UNEP): Nairobi, Kenya, 2012; pp. 1–24.
12. Santamouris, M. *Minimizing Energy Consumption, Energy Poverty and Global and Local Climate Change in the Built Environment: Innovating to Zero: Causalities and Impacts in a Zero Concept World*; Elsevier: Amsterdam, The Netherlands, 2019.
13. Agency, I.E.; Birol, F. *World Energy Outlook 2013*; International Energy Agency Paris: Paris, France, 2013.
14. Wang, Y.; Du, H.; Xu, Y.; Lu, D.; Wang, X.; Guo, Z. Temporal and spatial variation relationship and influence factors on surface urban heat island and ozone pollution in the Yangtze River Delta, China. *Sci. Total Environ.* **2018**, *631–632*, 921–933. [[CrossRef](#)]
15. Santamouris, M. *Energy and Climate in the Urban Built Environment*; CRC Press LLC: London, UK, 2001. [[CrossRef](#)]
16. Santamouris, M.; Cartalis, C.; Synnefa, A.; Kolokotsa, D. On the impact of urban heat island and global warming on the power demand and electricity consumption of buildings—A review. *Energy Build.* **2015**, *98*, 119–124. [[CrossRef](#)]
17. Santamouris, M. Cooling the buildings—past, present and future. *Energy Build.* **2016**, *128*, 617–638. [[CrossRef](#)]
18. Kovats, R.S.; Hajat, S.; Wilkinson, P. Contrasting patterns of mortality and hospital admissions during hot weather and heat waves in Greater London, UK. *Occup. Environ. Med.* **2004**, *61*, 893–898. [[CrossRef](#)]
19. Baccini, M.; Biggeri, A.; Accetta, G.; Kosatsky, T.; Katsouyanni, K.; Analitis, A.; Anderson, H.; Bisanti, L.; D’Ippoliti, D.; Danova, J.; et al. Heat Effects on Mortality in 15 European Cities. *Epidemiology* **2008**, *19*, 711–719. [[CrossRef](#)] [[PubMed](#)]
20. Goggins, W.; Chan, E.Y.; Ng, E.; Ren, C.; Chen, L. Effect Modification of the Association between Short-term Meteorological Factors and Mortality by Urban Heat Islands in Hong Kong. *PLoS ONE* **2012**, *7*, e38551. [[CrossRef](#)] [[PubMed](#)]
21. Mirzaei, P.; Haghghat, F. Approaches to study Urban Heat Island—Abilities and limitations. *Build. Environ.* **2010**, *45*, 2192–2201. [[CrossRef](#)]
22. Kato, S.; Yamaguchi, Y. Estimation of storage heat flux in an urban area using ASTER data. *Remote Sens. Environ.* **2007**, *110*, 1–17. [[CrossRef](#)]
23. Zhang, X.; Zhong, T.; Feng, X.; Wang, K. Estimation of the relationship between vegetation patches and urban land surface temperature with remote sensing. *Int. J. Remote Sens.* **2009**, *30*, 2105–2118. [[CrossRef](#)]
24. epa.gov. Heat Islands. Available online: <https://www.epa.gov/heat-islands/heat-island-compendium> (accessed on 12 June 2020).

25. Lazzarini, M.; Molini, A.; Marpu, P.; Ouarda, T.M.J.; Ghedira, H. Urban climate modifications in hot desert cities: The role of land cover, local climate, and seasonality. *Geophys. Res. Lett.* **2015**, *42*, 9980–9989. [CrossRef]
26. Lazzarini, M.; Marpu, P.; Ghedira, H. Temperature-land cover interactions: The inversion of urban heat island phenomenon in desert city areas. *Remote Sens. Environ.* **2013**, *130*, 136–152. [CrossRef]
27. Charabi, Y.; Bakhit, A. Assessment of the canopy urban heat island of a coastal arid tropical city: The case of Muscat, Oman. *Atmos. Res.* **2011**, *101*, 215–227. [CrossRef]
28. Radhi, H.; Fikry, F.; Sharples, S. Impacts of urbanisation on the thermal behaviour of new built up environments: A scoping study of the urban heat island in Bahrain. *Landsc. Urban Plan.* **2013**, *113*, 47–61. [CrossRef]
29. Al-Sallal, K.; Al-Rais, L. Outdoor airflow analysis and potential for passive cooling in the modern urban context of Dubai. *Renew. Energy* **2012**, *38*, 40–49. [CrossRef]
30. u.ae/en. about-the-uae/the-seven-emirates/dubai. Available online: <https://u.ae/en/about-the-uae/the-seven-emirates/dubai> (accessed on 23 May 2020).
31. dsc.gov.ae. Themes > Population and Vital Statistics. Available online: [https://www.dsc.gov.ae/en-us/Themes/Pages/Population-and-Vital-Statistics.aspx?Theme=42&year=2014#DSC\\_Tab1](https://www.dsc.gov.ae/en-us/Themes/Pages/Population-and-Vital-Statistics.aspx?Theme=42&year=2014#DSC_Tab1) (accessed on 20 March 2020).
32. weatherspark.com. Average Weather at Dubai International Airport United Arab Emirates. Available online: <https://weatherspark.com/y/148889/Average-Weather-at-Dubai-International-Airport-United-Arab-Emirates-Year-Round> (accessed on 20 March 2020).
33. ncm.ae. Radar UAE. Available online: [https://www.ncm.ae/en#!/Radar\\_UAE\\_Merge/26](https://www.ncm.ae/en#!/Radar_UAE_Merge/26) (accessed on 23 March 2020).
34. dubaidxbairport.com. Dubai International Airport. Available online: <https://www.dubaidxbairport.com/> (accessed on 27 March 2020).
35. cnbc.com. Dubai International Airport Installs 15,000 Solar Panels. Available online: <https://www.cnbc.com/2019/07/17/dubai-international-airport-installs-15000-solar-panels.html> (accessed on 27 March 2020).
36. fscloudport.com. Al Maktoum International Airport (OMDW). Available online: <http://www.fscloudport.com/atk/fscp.nsf/c9482105febd1beb802583bb006e932b/5f8ee3f40129ce9b802583bb006ec4f7?OpenDocument> (accessed on 1 April 2020).
37. dsc.gov.ae. Population Bulletin Emirate of Dubai 2018. Available online: <https://www.dsc.gov.ae/Publication/Population%20Bulletin%20Emirate%20of%20Dubai%202018.pdf> (accessed on 3 April 2020).
38. thenational.ae. Dubai Ruler launches Marmoom Desert Conservation Reserve. Available online: <https://www.thenational.ae/uae/environment/dubai-ruler-launches-marmoom-desert-conservation-reserve-1.696015> (accessed on 3 April 2020).
39. citypopulation.de. UAE: Division of Dubai. Available online: <https://www.citypopulation.de/en/uae/dubai/admin/> (accessed on 10 June 2020).
40. Camilloni, I.; Barrucand, M. Temporal variability of the Buenos Aires, Argentina, urban heat island. *Theor. Appl. Climatol.* **2011**, *107*, 47–58. [CrossRef]
41. von Glasow, R.; Jickells, T.; Baklanov, A.; Carmichael, G.; Church, T.; Gallardo, L.; Hughes, C.; Kanakidou, M.; Liss, P.; Mee, L.; et al. Megacities and Large Urban Agglomerations in the Coastal Zone: Interactions Between Atmosphere, Land, and Marine Ecosystems. *AMBIO* **2012**, *42*, 13–28. [CrossRef] [PubMed]
42. Yoshikado, H. Numerical Study of the Daytime Urban Effect and Its Interaction with the Sea Breeze. *J. Appl. Meteorol. (1988–2005)* **1992**, *31*, 1146–1164.
43. Dandou, A.; Tombrou, M.; Soulakellis, N. The Influence of the City of Athens on the Evolution of the Sea-Breeze Front. *Bound. Layer Meteorol.* **2008**, *131*, 35–51. [CrossRef]
44. Santamouris, M.; Papanikolaou, N.; Livada, I.; Koronakis, I.; Georgakis, C.; Argiriou, A.; Assimakopoulos, D.N. On the impact of urban climate on the energy consumption of buildings. *Sol. Energy* **2001**, *70*, 201–216. [CrossRef]
45. Sakaida, K.; Egoshi, A.; Kuramochi, M. Effects of Sea Breezes on Mitigating Urban Heat Island Phenomenon: Vertical Observation Results in the Urban Center of Sendai. *Jpn. Prog. Climatol.* **2011**, 11–16.
46. Erell, E.; Williamson, T. Intra-urban differences in canopy layer air temperature at a mid-latitude city. *Int. J. Climatol.* **2007**, *27*, 1243–1255. [CrossRef]
47. Anibaba, B.W.; Durowoju, O.S.; Adedeji, O.I. Assessing the Significance of Meteorological Parameters to the Magnitude of Urban Heat Island (Uhi). *Ann. Univ. Oradea, Geogr. Ser.* **2019**, *29*, 30–39. [CrossRef]

48. Ganbat, G.; Han, J.-Y.; Ryu, Y.-H.; Baik, J.-J. Characteristics of the urban heat island in a high-altitude metropolitan city, Ulaanbaatar, Mongolia. *Asia-Pac. J. Atmos. Sci.* **2013**, *49*, 535–541. [[CrossRef](#)]
49. Li, D.; Sun, T.; Liu, M.; Wang, L.; Gao, Z. Changes in Wind Speed under Heat Waves Enhance Urban Heat Islands in the Beijing Metropolitan Area. *J. Appl. Meteorol. Climatol.* **2016**, *55*, 2369–2375. [[CrossRef](#)]
50. Alonso, M.S.; Fidalgo, M.R.; Labajo, J.L. The urban heat island in Salamanca (Spain) and its relationship to meteorological parameters. *Clim. Res.* **2007**, *34*, 39–46. [[CrossRef](#)]
51. Sundborg, Å. Local Climatological Studies of the Temperature Conditions in an Urban Area. *Tellus* **1950**, *2*, 222–232. [[CrossRef](#)]
52. Papanikolaou, N.M.; Livada, I.; Santamouris, M.; Niachou, K. The Influence of Wind Speed on Heat Island Phenomena in Athens, Greece. *Int. J. Vent.* **2008**, *6*, 337–348. [[CrossRef](#)]
53. Sheng, L.; Tang, X.; You, H.; Gu, Q.; Hu, H. Comparison of the urban heat island intensity quantified by using air temperature and Landsat land surface temperature in Hangzhou, China. *Ecol. Indic.* **2017**, *72*, 738–746. [[CrossRef](#)]
54. Santamouris, M. On the energy impact of urban heat island and global warming on buildings. *Energy Build.* **2014**, *82*, 100–113. [[CrossRef](#)]
55. Liu, W.; Ji, C.; Zhong, J.; Jiang, X.; Zheng, Z. Temporal characteristics of the Beijing urban heat island. *Theor. Appl. Climatol.* **2006**, *87*, 213–221. [[CrossRef](#)]
56. Skoulika, F.; Santamouris, M.; Kolokotsa, D.; Boemi, N. On the thermal characteristics and the mitigation potential of a medium size urban park in Athens, Greece. *Landsc. Urban Plan.* **2014**, *123*, 73–86. [[CrossRef](#)]
57. Mihalakakou, G.; Flocas, H.A.; Santamouris, M.; Helmis, C.G. Application of Neural Networks to the Simulation of the Heat Island over Athens, Greece, Using Synoptic Types as a Predictor. *J. Appl. Meteorol. (1988–2005)* **2002**, *41*, 519–527. [[CrossRef](#)]
58. Santamouris, M. Analyzing the heat island magnitude and characteristics in one hundred Asian and Australian cities and regions. *Sci. Total Environ.* **2015**, *512–513*, 582–598. [[CrossRef](#)]
59. Schatz, J.; Kucharik, C. Urban climate effects on extreme temperatures in Madison, Wisconsin, USA. *Environ. Res. Lett.* **2015**, *10*, 094024. [[CrossRef](#)]
60. Lee, S.-H.; Baik, J.-J. Statistical and dynamical characteristics of the urban heat island intensity in Seoul. *Theor. Appl. Climatol.* **2010**, *100*, 227–237. [[CrossRef](#)]
61. Kim, Y.-H.; Baik, J.-J. Maximum Urban Heat Island Intensity in Seoul. *J. Appl. Meteorol. (1988–2005)* **2002**, *41*, 651–659. [[CrossRef](#)]
62. Yoshikado, H.; Tsuchida, M. High Levels of Winter Air Pollution under the Influence of the Urban Heat Island along the Shore of Tokyo Bay. *J. Appl. Meteorol.* **1996**, *35*, 1804–1813. [[CrossRef](#)]
63. Khan, S.; Simpson, R. Effect Of A Heat Island On The Meteorology Of A Complex Urban Airshed. *Boun. Layer Meteorol.* **2001**, *100*, 487–506. [[CrossRef](#)]
64. Freitas, E.; Rozoff, C.; Cotton, W.; Dias, P.S. Interactions of an urban heat island and sea-breeze circulations during winter over the metropolitan area of São Paulo, Brazil. *Bound. Layer Meteorol.* **2006**, *122*, 43–65. [[CrossRef](#)]
65. Ackerman, B. Temporal March of the Chicago Heat Island. *J. Clim. Appl. Meteorol.* **1985**, *24*, 547–554. [[CrossRef](#)]
66. Montávez, J.P.; Rodríguez, A.; Jiménez, J.I. A study of the Urban Heat Island of Granada. *J. R. Meteorol. Soc.* **2000**, *20*, 899–911. [[CrossRef](#)]
67. Camilloni, I.s.; Barros, V. On the Urban Heat Island Effect Dependence on Temperature Trends. *Clim. Chang.* **1997**, *37*, 665–681. [[CrossRef](#)]

